



**UNIVERSIDAD DE INVESTIGACIÓN DE TECNOLOGÍA  
EXPERIMENTAL YACHAY**

**Escuela de Ciencias Físicas y Nanotecnología**

**TÍTULO: Basic Molecular electronics through Break Junction  
measurements**

Trabajo de integración curricular presentado como requisito para la obtención de título de Físico

**Autor:**

Daniel Fernando Correa Rosales

**Tutor:**

Werner Bramer Escamilla, Ph.D

**Co-tutor:**

Ernesto Antonio Medina Dagger, Ph.D

Urququí, Octubre 2021

**SECRETARÍA GENERAL**  
**(Vicerrectorado Académico/Cancillería)**  
**ESCUELA DE CIENCIAS FÍSICAS Y NANOTECNOLOGÍA**  
**CARRERA DE FÍSICA**  
**ACTA DE DEFENSA No. UITEY-PHY-2022-00003-AD**

A los 29 días del mes de marzo de 2022, a las 11:00 horas, de manera virtual mediante videoconferencia, y ante el Tribunal Calificador, integrado por los docentes:

<b>Presidente Tribunal de Defensa</b>	Dr. REINOSO CARLOS , Ph.D.
<b>Miembro No Tutor</b>	Dr. GUEVARA GRANIZO, MARCO VINICIO , Ph.D.
<b>Tutor</b>	Dr. BRAMER ESCAMILLA , WERNER , Ph.D.

El(la) señor(ita) estudiante **CORREA ROSALES, DANIEL FERNANDO**, con cédula de identidad No. **1722955430**, de la **ESCUELA DE CIENCIAS FÍSICAS Y NANOTECNOLOGÍA**, de la Carrera de **FÍSICA**, aprobada por el Consejo de Educación Superior (CES), mediante Resolución **RPC-SO-39-No.456-2014**, realiza a través de videoconferencia, la sustentación de su trabajo de titulación denominado: **Basic molecular electronics through break junction measurements**, previa a la obtención del título de **FÍSICO/A**.

El citado trabajo de titulación, fue debidamente aprobado por el(los) docente(s):

<b>Tutor</b>	Dr. BRAMER ESCAMILLA , WERNER , Ph.D.
<b>Co - Tutor</b>	Dr. MEDINA DAGGER, ERNESTO ANTONIO , Ph.D.

Y recibió las observaciones de los otros miembros del Tribunal Calificador, las mismas que han sido incorporadas por el(la) estudiante.

Previamente cumplidos los requisitos legales y reglamentarios, el trabajo de titulación fue sustentado por el(la) estudiante y examinado por los miembros del Tribunal Calificador. Escuchada la sustentación del trabajo de titulación a través de videoconferencia, que integró la exposición de el(la) estudiante sobre el contenido de la misma y las preguntas formuladas por los miembros del Tribunal, se califica la sustentación del trabajo de titulación con las siguientes calificaciones:

Tipo	Docente	Calificación
Tutor	Dr. BRAMER ESCAMILLA , WERNER , Ph.D.	10,0
Miembro Tribunal De Defensa	Dr. GUEVARA GRANIZO, MARCO VINICIO , Ph.D.	9,5
Presidente Tribunal De Defensa	Dr. REINOSO CARLOS , Ph.D.	8,6

Lo que da un promedio de: **9.4 (Nueve punto Cuatro)**, sobre 10 (diez), equivalente a: **APROBADO**

Para constancia de lo actuado, firman los miembros del Tribunal Calificador, el/la estudiante y el/la secretario ad-hoc.

*Certifico que en cumplimiento del Decreto Ejecutivo 1017 de 16 de marzo de 2020, la defensa de trabajo de titulación (o examen de grado modalidad teórico práctica) se realizó vía virtual, por lo que las firmas de los miembros del Tribunal de Defensa de Grado, constan en forma digital.*

CORREA ROSALES, DANIEL FERNANDO  
**Estudiante**

Dr. REINOSO CARLOS , Ph.D.  
**Presidente Tribunal de Defensa**

Dr. BRAMER ESCAMILLA , WERNER , Ph.D.  
**Tutor**

Dr. GUEVARA GRANIZO, MARCO VINICIO , Ph.D.  
**Miembro No Tutor**

CIFUENTES TAFUR, EVELYN CAROLINA  
**Secretario Ad-hoc**

## AUTORÍA

Yo, **Daniel Fernando Correa Rosales**, con cédula de identidad 1722955430, declaro que las ideas, juicios, valoraciones, interpretaciones, consultas bibliográficas, definiciones y conceptualizaciones expuestas en el presente trabajo; así como, los procedimientos y herramientas utilizadas en la investigación, son de absoluta responsabilidad de el/la autora (a) del trabajo de integración curricular. Así mismo, me acojo a los reglamentos internos de la Universidad de Investigación de Tecnología Experimental Yachay.

*Urcuquí, Octubre 2021*

---

Daniel Fernando Correa Rosales

## **AUTORIZACIÓN DE PUBLICACIÓN**

Yo, **Daniel Fernando Correa Rosales**, con cédula de identidad **1722955430**, cedo a la Universidad de Investigación de Tecnología Experimental Yachay, los derechos de publicación de a presente obra, sin que deba haber un reconocimiento económico por este concepto. Declaro además que el texto del presente trabajo de titulación no podrá ser cedido a ninguna empresa editorial para su publicación u otros fines, sin contar previamente con la autorización escrita de la Universidad.

Asimismo, autorizo a la Universidad que realice la digitalización y publicación de este trabajo de integración curricular en el repositorio virtual, de conformidad a lo dispuesto en el Art. 144 de la Ley Orgánica de Educación Superior

*Urcuquí, Octubre 2021*

---

Daniel Fernando Correa Rosales

# Abstract

Molecular electronics (ME) is an emerging technology that studies the electronic and thermal transport properties of individual molecules for the development of new devices with a very reduced size. Every metallic material and molecule has its own conductance value, so it is important to understand the conductance of a specific molecule. In this work we performed the molecular quantum conductance measurements of a benzene molecule, using a Mechanically Controlled Break Junction (MCBJ). To perform the conductance quantization of a benzene molecule it is needed to first perform the calibration of the equipment, make the conductance measurements of clean gold junction and then place a drop of a benzene solution in the junction. Then around  $\sim 2000$  traces are collected to build the conductance histogram to observe the quantum characteristic conductance peak of a benzene molecule. By analyzing the histograms obtained from this experiment it is observed that the benzene molecule has the characteristic of shifting the gold peak to the right and has its first conductance peak located at  $-0.30 \text{ Log}(G_0)$ . From this results it can be concluded that the MCBJ equipment has the enough resolution to detect the presence of a benzene molecule and measure its conductance.

**Keywords:** Molecular electronics (ME), conductance quantization, nano-contact, Mechanically Controlled Break Junction (MCBJ), conductance histogram, gold electrodes, benzene.



# Resumen

La Electrónica Molecular (ME) es una tecnología en desarrollo que estudia el transporte eléctrico y térmico de moléculas individuales para el desarrollo de nuevos dispositivos con un tamaño reducido. El valor de la conductancia es específico para cada metal y molécula, por eso es importante el estudio de la conductancia para cada molécula. En este trabajo se realizó el estudio de la conductancia molecular para una molécula de benceno usando Mechanically Controlled Break Junction (MCBJ). Para realizar las mediciones de la cuantización de la conductancias de una molécula de benceno se tuvo que calibrar el equipo, hacer mediciones de conductancia de un alambre de oro limpio y después se colocó una gota de una solución de benceno en la unión de los electrodos de oro. Luego se recolectaron alrededor de  $\sim 2000$  trazas para realizar el histograma de conductancia y observar los picos característicos de una molécula de benceno. Después de analizar los histogramas se obtuvo que el benceno tiene la característica de trasladar el pico de conductancia del oro hacia la derecha y además se puede observar un pico característico de conductancia en  $-0.30 \text{ Log}(G_0)$ . Con estos resultados se puede concluir que el equipo MCBJ tiene la resolución necesaria para detectar la presencia de benceno y medir su conductancia.

**Palabras clave:** Electrónica Molecular (ME), cuantización de la conductancia, nano contacto, Mechanically Controlled Break Junction (MCBJ), histograma de conductancia, electrodos de oro, benceno.



# Acknowledgments

I would like to thank both of my advisors, Werner Bramer and Ernesto Medina, for their help and guidance that made possible the development of this thesis project. Additionally, I would like to thank to Carlos Sabater for his help and guidance during his visit to Ecuador, without him this project would have being much harder. Also, I would like to thank to my parents and sisters for their support through all the years of my career. I would like to thank to the professors that gave me classes and passed their knowledge since the beginning of my career, from leveling course to my graduation. At the same time I am grateful to all the professors that are part of Yachay Tech, for always believing in their students and never giving up in spite all difficulties, without them the university would never have existed. Finally, I would like to thank to friends and all the people that I met during my career that made Yachay Tech my second home.

Daniel Fernando Correa Rosales

# Contents

<b>List of Figures</b>	<b>xiv</b>
<b>List of Tables</b>	<b>xv</b>
<b>1 Introduction</b>	<b>1</b>
1.1 Experimental methods to address ME . . . . .	2
1.1.1 Scanning probe . . . . .	3
1.1.2 Fixed electrodes . . . . .	3
1.1.3 Mechanically Formed Molecular Junctions . . . . .	4
1.1.4 The future of ME . . . . .	7
1.2 The MCBJ technique . . . . .	7
1.3 Objectives . . . . .	10
1.3.1 General objective . . . . .	10
1.3.2 Specific objectives . . . . .	10
1.4 Overview . . . . .	11
<b>2 Theoretical Background</b>	<b>13</b>
2.1 Conductance quantization . . . . .	13
2.1.1 Landauer formula heuristic derivation . . . . .	15
2.2 Solution to the simple problem for a quasi 1D metallic junction . . . . .	18
2.2.1 Conductance histograms . . . . .	20
2.3 Spin degree of freedom, ferromagnetic junctions . . . . .	22
2.3.1 Conductance on ferromagnetic atomic contacts . . . . .	22
2.4 Molecular junctions . . . . .	23
2.4.1 Coherent transport through molecular junctions . . . . .	26

2.4.2	Length dependence on the conductance . . . . .	27
<b>3</b>	<b>Experimental Methodology</b>	<b>29</b>
3.1	State of the art of MCBJ . . . . .	29
3.2	Mechanics and electronics of the MCBJ . . . . .	33
3.3	Conductance measurements . . . . .	35
3.3.1	Sample preparation . . . . .	35
3.4	Measurement of the resolution of the MCBJ . . . . .	35
3.5	Proposed experimental developments . . . . .	38
3.6	Reference molecules measurement expectations . . . . .	38
<b>4</b>	<b>Results &amp; Discussion</b>	<b>41</b>
4.1	Tight binding model . . . . .	41
4.1.1	Cyclic molecule: benzene . . . . .	42
4.1.2	Transmission of a benzene molecule . . . . .	44
4.2	Experimental measurements . . . . .	52
4.2.1	Metallic measurements . . . . .	52
4.2.2	Molecules measurements . . . . .	54
<b>5</b>	<b>Conclusion &amp; Recommendations</b>	<b>57</b>
	<b>Bibliography</b>	<b>59</b>
	<b>Abbreviations</b>	<b>63</b>

# List of Figures

1.1	Interdisciplinary of ME. Adapted from <sup>1</sup> . . . . .	2
1.2	Scanning probe technique using a Scanning Tunneling Microscopy (STM) or Atomic Force Microscope (AFM). Adapted from <sup>2</sup> . . . . .	3
1.3	Techniques using fixed electrodes approaches. Left, molecule bridged between two electrodes; separation gap is made using electromitigation, electrochemical etching or deposition. Middle, Bridging between the molecules using a metal particles. Right, dimer structure made of two Au particles bridged with a molecule. Pictures taken from <sup>2</sup> . . . . .	4
1.4	MCBJ technique scheme. Figure taken from <sup>2</sup> . . . . .	5
1.5	STM technique scheme. Figure taken from <sup>2</sup> . . . . .	6
1.6	AFM technique scheme. Figure taken from <sup>2</sup> . . . . .	6
1.7	Left image, MCBJ principle setup. Right image, electron micrograph of a thin film MCBJ. Figures taken from <sup>1</sup> . . . . .	9
2.1	Schematic illustration of conductance in metallic contacts, a) diffusive, b) ballistic, c) quantum. Adapted from <sup>1,3</sup> . . . . .	14
2.2	Wave function representation when impinging a potential barrier. The wave is partially reflected with an amplitude $r$ and partially transmitted with and amplitude $t$ . Retrieved from <sup>1</sup> . . . . .	15
2.3	Graphical representation of $f_L(E) - f_R(E)$ at low temperature. . . . .	18
2.4	Recording of conductance $G$ measured in atomic contacts for gold using MCBJ. Retrieved from <sup>1</sup> . . . . .	20
2.5	In the left picture it can seen the evolution of the atomic rearrangements during the stretching of the wire. In the right picture it can be seen the conductance measurements and the channel contribution along the stretching path. Retrieved from <sup>1</sup> . . . . .	21
2.6	Gold conductance histogram.Retrieved from <sup>4</sup> . . . . .	22

2.7	Iron conductance histogram measured at 10 K. Adapted from <sup>5</sup> . . . . .	23
2.8	Conductance histograms for Fe, Co and Ni obtained by applying a magnetic field (thick curve) and without applying a magnetic field (thin curve). This measurements were performed at a temperature of 4.2 K. Retrieved from <sup>1</sup> . . . . .	24
2.9	Iron conductance histogram measured at 10 K. Adapted from <sup>5</sup> . . . . .	24
2.10	Iron conductance histogram measured with magnetically saturated wires. Retrieved from <sup>6</sup> . . . . .	25
3.1	Gold metal wire for the construction of the electrodes with an ultra-high purity of 99.999%. . . . .	29
3.2	MCBJ main head. . . . .	30
3.3	Fully assembled MCBJ. . . . .	31
3.4	Fast electronics equipment. Left: bias voltage ( $V_{bias}$ ) controller, in this experiment is set to 100mV . Right: piezocontroller from Thorlabs, used for up and down movement of the piezoelectric. . . . .	31
3.5	Fast electronics equipment. Left: Oscilloscope. Center: I/V preamplifier, in this experiment for metallic junction amplifies the signal $10^5$ and for molecules $10^6$ . Right: data acquisition (DAQ) from Measurement Computing, model USB-1808X, with a resolution of 18 bits and a max sample rate of 200 KS/s. . . . .	32
3.6	Complete MCBJ equipment. . . . .	32
3.7	Left: wire slicing device to make a groove with a diameter of 1/3 of the original width of the wire. Right: stereoscopic magnifier. . . . .	33
3.8	Circuit diagram with the components and the connection of the MCBJ. . . . .	34
3.9	Program built in LabVIEW by Werner Bramer and Carlos Sabater for making the measurements. Top: program used to save the traces measured in the MCBJ. Bottom: program that controls the up and down movement of the piezoelectric. . . . .	34
3.10	Sample preparation process. 1) Straightening of the wire between two microscope slides. 2) Creation of the groove in the wire using the device shown in Fig. 3.7. 3) Grooved wire in the piranha solution. 4) Fixing the gold wire on the substrate covered with Kapton tape with nail polish. 5) Placing two drops of epoxy adhesive at each side of the groove with a triangular shape. 6) Placing the substrate in the sample holder and making the connections using silver paste. Steps 5) and 6) are performed under the stereoscopic magnifier. . . . .	36
3.11	Sample preparation. Left: gold wire with the groove. Center: gold wire with the epoxy adhesive in triangular shape. Right: substrate ready to be placed in the sample holder. . . . .	36
3.12	Left: sample ready. Right: sample placed in the MCBJ. . . . .	37

3.13	Resolution of the MCBJ. . . . .	37
4.1	Left: scheme of a benzene molecule used to calculate the electronic structure using simple tight binding model. Right: energy levels diagram of benzene, obtained using this approximation; we have a Highest occupied molecular orbital (HOMO)-lowest unoccupied molecular orbital (LUMO) gap equal to $2t$ and a total energy $E_T = 6\epsilon_0 - 8t$ . Adapted from <sup>1</sup> . . . . .	42
4.2	Benzene coupling configurations between two semi-infinite electrodes with gold parameterization. In para (left), meta (center) and ortho (right) configurations. . . . .	47
4.3	The plot shows the transmission through the benzene in the parallel configuration for the three different couplings. The light yellow region depicts the bandwidth of the gold contacts where transmission can occur. We see a concentration of the transmission around the LUMO level of the molecule widened and shifted by the self energy of the contracts. There are only slight differences between the orto, para and meta configurations. The centers of the input and output bands differ by 1 meV. In this model the transmittance was caluclated by making the contact of the infinite gold chain on an individual carbon atom, which is represented as the blue line. Then total transmittance is calculated by summing up the transmittance contribution of the 6 carbon atoms, which is represented as the dark blue line. . . . .	48
4.4	The plot shows the transmission through the benzene in the perpendicular configuration for a symmetric coupling to all carbons. . . . .	49
4.5	Benzene transmittance in perpendicular configuration. The light yellow region depicts the bandwidth of the gold contacts where transmission can occur. We see a concentration of the transmission around the LUMO level of the molecule widened and shifted by the self energy of the contacts. The centers of the input and output bands differ by 1 meV. The transmittance for this model was done by attaching the semi-infinite gold electrodes to an individual carbon atom, this individual transmittance is represented by the blue line. Then the total transmittance is calculated by summing up the transmittance of the 6 carbon atoms, which is represented by the thicker dark blue line. . . . .	50

4.6	Comparison of benzene transmittance in perpendicular and parallel configurations. It can be observed that the transmittance in the perpendicular (green) configuration is higher than the transmittance in parallel (blue) configuration. Another observation that can be conclude is that the range of energy for the transmittance to occur is higher in the perpendicular configuration. . . . .	51
4.7	Example of gold conductance traces made at room temperature. The signal is amplified $10^5$ times. . . . .	53
4.8	Gold conductance histogram. . . . .	53
4.9	Gold conductance histogram amplifying the signal $10^6$ times. To be able to distinguish low conductance values the conductance values and the counts of the histogram are plotted in logarithmic scale. . . . .	54
4.10	Comparison of clean Gold and Gold-benzene conductance histogram. . . . .	55

# List of Tables

2.1	Molecular junction conduction mechanisms. Retrived from <sup>1</sup> . . . . .	26
3.1	Expected conductance benzene molecules de Ara <i>et al.</i> <sup>7</sup> . . . . .	39





# Chapter 1

## Introduction

Molecular electronics (ME) is the field of science that studies the electronic and thermal transport properties of individual molecules for the construction of new devices with a very reduced size<sup>1</sup>. There exist molecules with unique functions that may have many applications that are complementary to the silicon based microelectronics. Scientist have found that molecules with very interesting electronic properties and there have being others synthesized with additional desired characteristics like for example: optical, magnetic, thermoelectric, electromechanical and molecular recognition properties. By understanding these characteristics of molecules we may be able to develop new devices that would not be possible using conventional materials approaches<sup>2</sup>. ME is an interdisciplinary field that merges physics, chemistry, biology, electronics and information technology<sup>8</sup>.

There have being several important advances that have improved our understanding of this field. The advances are: demonstration of simple molecular device functions, developments of different experimental approaches for measuring electron transport in single molecules and theoretical methods for describing the electron transport properties, development of new characterization techniques that help to connect theoretical and experimental approaches, and the development of hybrid devices which have been actively pursued to the efforts of pure electronic devices<sup>2</sup>.

ME offers advantages in size, speed, assembly, recognition, new functionalities and synthetic tailorability<sup>1</sup>. The reduction in size leads toward a higher packing density of devices, which will improve the cost, efficiency and power dissipation. Good molecular wires can reduce the transit time of transistors, to around  $10^{-14}$  s, reducing the time needed for device operations. Assembly of molecules takes advantage of

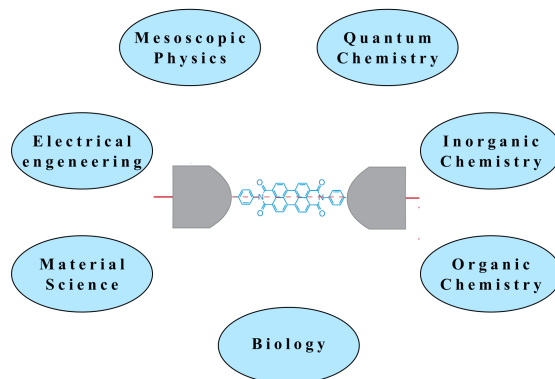


Figure 1.1: Interdisciplinary of ME. Adapted from<sup>1</sup>

specific inter-molecular interactions to form structures by nanoscale self-assembly<sup>1</sup>. Molecular recognition could also be used to modify electronic behavior, providing switching and sensing capabilities. Molecules' special properties, like the existence of distinct stable geometric structures, lend themselves to finding new electronic functions. Exploring molecules' composition and geometry, can vary the molecule's transport, binding, optical and structural properties<sup>1</sup>. One thing that is important to be taken into account is that at the molecular scale, charge transport is governed by the anchoring groups of the molecule, the properties of the orbitals bearing mobile electron and the connecting electrodes<sup>9</sup>.

In order to understand charge transport, it is really important to be able to measure and control the electrical current through a molecule. Charge transfer is an important phenomenon that occurs in many chemicals with functionalities in biological processes such as photosynthesis, cellular reparations, DNA repair, magnetic field sensing, etc<sup>10</sup>. An important application to understand the characteristics of charge transport in single molecules is that we might be able to investigate biosensor applications based on the electrical detection of individual molecular binding events<sup>11</sup>.

## 1.1 Experimental methods to address ME

To determine the conductance of a single molecule, we must provide three things: first a signature to identify that the measured conductance is a result of a single sample molecule, second we have to ensure

that the molecule is properly attached to the two probing electrodes, and third perform the measurement in a well-defined environment. The current methods for the measurements fall into three categories: scanning probe methods, fixed electrodes, and mechanically controlled break junctions<sup>11</sup>.

### 1.1.1 Scanning probe

To perform measurements using the scanning probe technique we may use Scanning Tunneling Microscopy (STM) or an Atomic Force Microscope (AFM) with a conducting tip. The STM has played a unique role in this field because it allows imaging individual molecules adsorbed on the surface with sub-molecular resolution. This technique also allows performing tunneling spectroscopy measurements. Another advantage of this technique is that we are able to manipulate atoms and molecules on the surface. The AFM is a similar technique but the measurements have a lower resolution. When we are making measurements using these techniques, a molecule adsorbs onto a substrate, and then we approach the tip of the STM or AFM to the molecule we want to measure. The problem of this is that the tip-molecule contact is not well-defined, so the conductance measurements are not absolute. To solve this problem we perform three approaches. The first approach would be to embed the molecule we want to measure into a matrix of another less conducting molecules. The second approach would be to attach one end of the molecule to a step edge on a metal substrate. Finally, the third approach would be to attach one end of the molecule onto a substrate and the other end to a gold nanoparticle<sup>11</sup>

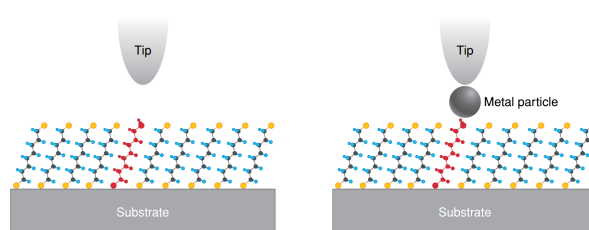


Figure 1.2: Scanning probe technique using a STM or AFM. Adapted from<sup>2</sup>

### 1.1.2 Fixed electrodes

This method consists in fabricating a pair of facing electrodes on a solid substrate and then connecting them with a molecule terminated with the proper anchoring groups. The advantages of this technique are

that the fixed electrodes provide a stable molecular junction, which allow the study of electron transport as a function of temperature, magnetic field, etc. Another advantage is that we can use the substrate as gate electrode to control the electron transport through the molecule. The problem of this technique is that is difficult to fabricate electrodes with a proper molecular gap, with the size of a single molecule which is of a few nanometers. The methods used to solve this problem are described below. One technique is to create the gap using electromitigation, electrochemical etching or deposition. Another technique is to use connect the molecules using metal nanoparticles. When using this technique we have to cover both electrodes with the sample molecules of both electrodes, the to fill the gap, we place a metal nanoparticle with a bigger diameter than the gap. Using this technique we create two metal-molecule-metal junction in series. Another approach using nanoparticles is creating a dimer structure by placing two gold nanoparticles on the electrodes connected by a dithiolated organic molecule<sup>11</sup>

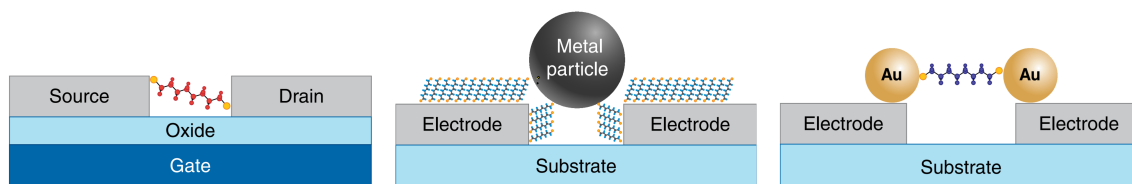


Figure 1.3: Techniques using fixed electrodes approaches. Left, molecule bridged between two electrodes; separation gap is made using electromitigation, electrochemical etching or deposition. Middle, Bridging between the molecules using a metal particles. Right, dimer structure made of two Au particles bridged with a molecule. Pictures taken from<sup>2</sup>.

### 1.1.3 Mechanically Formed Molecular Junctions

The difficulty to fabricate electrodes that are separated the exact length for every single molecule can be fixed by separating the electrodes mechanically until there is only one molecule making the junction. By using a Piezoelectric Transducer (PZT) we can control the gap between electrodes with a sub-angstrom precision, making it possible to measure the conductance of different molecules with different lengths<sup>11</sup>. The techniques used following this approach are the Mechanically Controlled Break Junction (MCBJ), STM based break junction and conducting AFM break junction.

## MCBJ

The basic idea of this technique is to break a thin metal wire into a pair of facing electrodes. One way to achieve this is to bend the substrate in a controlled way by using a PZT and a stepping motor. After we have the electrodes we can place a solution of the molecules we want of measure and let the molecules adsorb onto the electrodes. After this the gap between the electrodes is opened, while a fixed voltage is applied and the current is recorded. When the current reaches a stable value the separation between electrodes is stopped, and we can create I-V curves to understand the behavior of the molecule<sup>11</sup>.

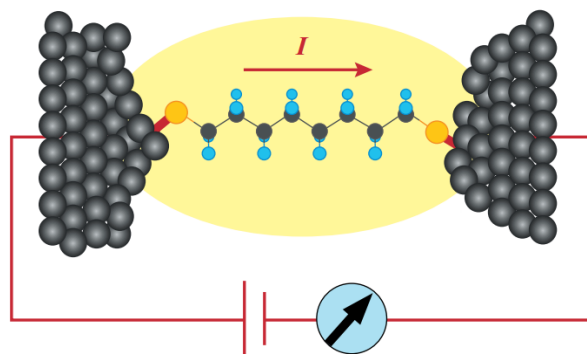


Figure 1.4: MCBJ technique scheme. Figure taken from<sup>2</sup>

## STM based break junction

The main idea of this technique is to repeatedly create and break contact between the tip of the STM and the substrate electrode in the presence of substrate electrodes. For the molecules to be able to bind to the tip, they have proper end groups. The measurement process is divided in two steps: First a PZT drives the tip towards the substrate to make contact with the molecules. Then the tip is pulled away and the molecules start to break contact with one of the two electrodes, which can be seen by step-wise decrease in the current. This process is repeated until a large amount of molecular junctions are created and measured, to build a conductance histogram and identify a single molecule conductance. This technique focuses on the separation of electrodes instead of the approaching<sup>11</sup>.

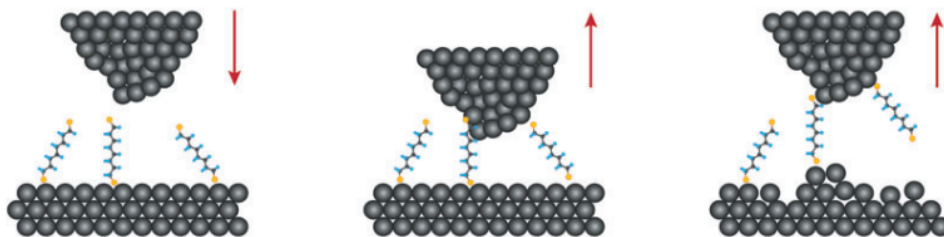


Figure 1.5: STM technique scheme. Figure taken from<sup>2</sup>

### Conducting AFM break junction

When using this technique we are able to measure the electromechanical properties of molecular junctions. From every decrease in the conductance we are also able to measure an abrupt decrease in the force, which corresponds to the breakdown of the contact between the molecule and the tip of the AFM. When the tip is pulled apart there is a slight change in the conductance and a approximate linear increase in the force until the abrupt decrease when the contact is broken<sup>11</sup>.

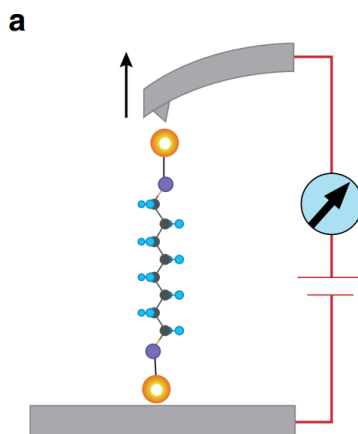


Figure 1.6: AFM technique scheme. Figure taken from<sup>2</sup>

### 1.1.4 The future of ME

ME can have many application in the electronics industry. The research in ME is done to find molecules that can function as switches and wires. Saxena and Malhotra<sup>8</sup> have studied Conducting Polymers (CPs) that can have metallic conductivity like polythiazil. They have also found other molecules that can be tuned from insulating to superconducting regime by doing chemical modifications. Other CPs can have behaviors of metal and semiconductor where the electronic properties is completely different than conventional semiconductors. Other advantages these polymers are that they are: lightweight, flexible, corrosion resistant, have high chemical inertness, can offer electrical insulation and are easy to process<sup>8</sup>.

Another application could be for studying the spintronic properties of certain molecules. Spintronics is the field of science that studies the intrinsic angular momentum (spin) of electrons<sup>12</sup> by controlling and manipulating the spin's degrees of freedom in solid state materials<sup>13</sup>. The spin of an electron could be pointing up or down<sup>12</sup>. The spin direction carry encoded information that can interact differently with magnetic fields. The advantages of this encoded information can persists even when the device is turned off, can be manipulated without using magnetic fields and can be written using low energies<sup>14</sup>. By controlling the spin direction scientists have being able to develop very important technological devices, like for example: computer hard drives, Random Access Memory (RAM), spin transistors and spin lasers<sup>12</sup>. By combining the ideas of spintronics and molecular electronics the new field of molecular spintronics is emerging, where the ideas and advantages of this two fields are combined. Scientist are working in the development of molecular devices using one or few magnetic molecules, which have the advantage that have very long relaxation time at low temperatures. In future technologies this magnetic molecules could be used for the development of high density information technology and for quantum computing due to their long coherence times<sup>14</sup>.

## 1.2 The MCBJ technique

In this work the measurement of electron transport in molecules will be done using the MCBJ technique. The device that is used was constructed at Yachay Tech University. This the first instrument of this kind completely build in Latin America. The design is based on that of Oren tal's group in Israel, which is one of the leaders in molecular electronics.

Conductance measurements have been applied to analyze the charge transport mechanism in single molecular junctions. According to Wang *et al.*<sup>15</sup> some parameters that may affect the conductance mea-



measurements are: the anchoring groups (connect the molecule to the electrodes), the molecular backbone (the molecule we are measuring without the anchoring groups) and the electrode material.

The anchoring groups are the interfaces between the molecules and the microscopic electrodes. They are of vital importance in the formation of stable single molecular junctions. An ideal anchoring group should possess three essential features: stable binding, high junction formation probability and high conductance. The charge transport mechanism are affected by different anchoring groups. The coupling strength between the molecule and the electrodes is dependent on the different anchoring groups. Another important feature of the coupling strength is that it governs the transition from coherent to incoherent transport. Besides controlling the coupling strength to determine the junction conductance, the anchoring groups also control the position of the relevant molecular energy levels. The anchoring groups are selected according to the formation of donor-acceptor bonds with the electrodes, according to their: contact resistance, forming possibility and stability, which are the factors that determine the conductance value. Some of the used anchoring groups have been: thiol ( $-SH$ ), amine ( $-NH_2$ ), carboxy acid ( $-COOH$ ), fullerenes ( $C_{60}$ ), etc. From all the anchoring groups, the most commonly used to connect gold electrodes with the target molecules are the thiol groups ( $-SH$ ). The reasons for this is that thiol groups can bond covalently to gold electrodes, making the Au-S bond stronger than the Au-Au bond<sup>15</sup>.

The molecular backbone play the role of a wire like structure. The molecular backbone studies investigate the development of single molecule functional devices, such as rectifiers, diodes, switchers, etc. It has been observed that that electron transport in the molecular backbone is dependent on the molecule's length. For small molecules the occurs due to non-resonant tunneling. As the length of the molecule increases to a certain value, the charge transport switches to charge hoping. It has been observed that when charge transport is governed by non-resonant tunneling there is a dependence on the length. While when it is dominated by charge hoping, charge transport is dependent on the temperature and weakly dependent on the length. For a certain types of molecules, it has been observed that there is an exponential decay as the molecular length increases until they reach a certain length. When the molecules becomes large enough the conductance still declines but at a slower rate<sup>15</sup>.

The electrode material plays an important role in the charge transport of single molecular orbitals. The electrode can be constructed with metals, carbon based molecules and also scientist have been studying the use of semiconductors. The metallic electrodes can be made of Au, Ag, Cu, Pt and Pb. From this materials Au is the most common used material as a metallic electrode. The reason for this is it possesses high

junction probability, chemical stability and electrical conductivity. The carbon based molecules that have been found to have excellent conductivity are Single Walled Carbon Nanotubes (SWCNTs) and graphene. All carbon based molecules have demonstrated extraordinary stability under extreme bias and thermal changes. Another material that is being used as charge transport measurement is the Silicon electrode. The advantages of this material is its high conductance and the ability to tune its Fermi level by doping<sup>15</sup>.

The MCBJ technique is a tool that is used to control and study single molecular junctions. The MCBJ measurement setup is divided in three sections: the pushing rod which responsible for creating the nanogap between the electrodes for making the measurements, a flexible substrate with the nanostructures we want to measure that can be made of silicon, spring steel or phosphor bronze and two lateral supports to exert a force in the central point of the flexible substrate. The basic working principle is that exerts a force in the central part of the flexible substrate and the two lateral supports exert a force to the bendable substrate to hold it in place. The movement of the pushing rod is controlled by a mechanical actuator, such as a stepping motor or a piezo element<sup>15</sup>.

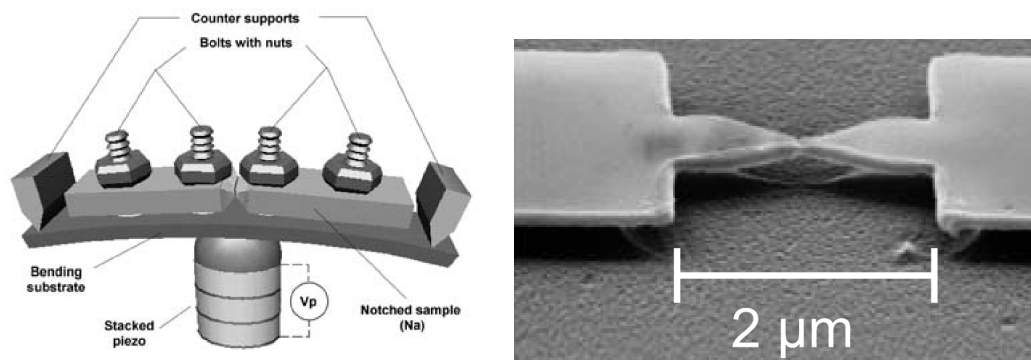


Figure 1.7: Left image, MCBJ principle setup. Right image, electron micrograph of a thin film MCBJ. Figures taken from<sup>1</sup>

The working principle of the MCBJ technique is the following. The pushing rod drives an upward force that cause the substrate bending, stretching the metal wire. As the metal wire keeps elongating, the central section is scaled down until its fracture, at this point a nanogap is created between two metal electrodes at the atomic level where clean surfaces are generated. If the surface is relaxed the two electrodes join together forming the original wire. The nanogap is controlled by bending and relaxing the substrate. To

promote insertion of the molecules in the gap a bias voltage is applied within the range of 80 – 330 mV. To have a very good coupling efficiency between the electrode and the molecules is necessary to set the gap length slightly longer than the length of the molecules<sup>15</sup>.

The MCBJ offers several advantages that makes it a good technique for studying the electrons transport in molecules. The first advantage is that it generates clean facing electrodes where there is a very weak influence of contaminants. Also the breaking and linking of the electrodes facilitates the collection of more experimental data to decrease data discretization in dynamic configurations. The third advantage is that this technique is very stable in the whole temperature range and on disruptive factors such as external vibrations, thermal drifts and the continuous motion of the pushing rod. The fourth advantage is that this technique can be easily combined with other techniques, such as inelastic tunneling spectroscopy, Surface-enhanced Raman Scattering (SERS), and electrochemical deposition<sup>15</sup>.

As every technique the MCBJ also has some disadvantages. One of them is that we cannot use it to obtain the evolution of the tip atoms in the formation of single molecular junctions. Another disadvantage is that is not convenient to add a gate electrode in a solid state which can be done in the electromitigation technique. The last disadvantage described by Wang *et al.*<sup>15</sup> is that the sites where the molecules are inserted is unknown which limits the explorations of the influence factor of the conductance<sup>15</sup>.

## 1.3 Objectives

### 1.3.1 General objective

- Perform a conductance measurement of an organic molecule by using the equipment MCBJ from the school of Physics and Nanotechnology

### 1.3.2 Specific objectives

- Transmittance calculation using a tight binding model for the benzene molecule.
- Perform measurements of conductance in gold electrodes.
- Measure the actual resolution of the equipment to determine what kind of molecules is able to measure.
- Perform conductance measurements from benzene molecules.

## 1.4 Overview

This work presented a small introduction of ME, some of the main techniques used in this field and some interesting prospects in the future, like spintronics. It also presented the MCBJ technique which is the one that is going to be used, with its advantages and disadvantages. In the next chapter, it will discuss the conductance quantization, present the solution for a quasi 1D metallic junction, explain about the spin degree of freedom in ferromagnetic junctions. Additionally, it will present the tight binding model for a benzene. The next chapter will explain the methodology of this work. It will start by explaining the equipment used in this work, mechanically and electronically. Then it will explain how the conductance measurements for the electrodes and the molecules are going to be performed. Finally, it will present some reference measurements of molecules that will be done. In the last section I will present the results of the conductance in gold wires and from the proposed molecules. The next chapter will show the results obtained by measuring the conductance of clean gold electrodes and when a drop of benzene is placed in the electrodes.



## Chapter 2

# Theoretical Background

### 2.1 Conductance quantization

On bulk materials, Ohm's law establishes that the current is proportional to the applied voltage,  $I \propto V$ . Where the proportionality constant is the conductance,  $G$ . The conductance is the fundamental quantity that describes the electronic transport in a material, which is defined as:

$$G = \sigma \frac{A}{L}, \quad (2.1)$$

where  $L$  is the length,  $A$  is the cross-sectional area of the material and  $\sigma$  is the conductivity. The conductivity is the fundamental quantity specific for each material, that describes the electrical properties of a material<sup>11</sup>. The conductance can be defined from Ohm's law as:

$$G = \frac{1}{R} = \frac{I}{V}. \quad (2.2)$$

From Eq. 2.1 and Eq. 2.2 the conductivity can be defined as:

$$\sigma = \frac{I}{V} \times \frac{L}{A}. \quad (2.3)$$

Since  $A$  and  $L$  are difficult to be defined precisely in individual molecules, the fundamental quantity that describes electronic transport is the conductance, Eq. 2.2.

On atomic size contacts is not so simple to use Ohm's law to measure the conductance. Atomic sized conductors are a limiting case of mesoscopic systems in which quantum coherence plays a central role in the transport properties. In mesoscopic systems conductance can be classified according to different transport regimes according to the relative size of various length scales, in these systems the conductance

depends on the relative sizes of width  $w$  and the length  $L$  of the contact compared with the mean free path  $l$ , which is defined as the average distance that an electron travels between successive collisions with static impurities<sup>3</sup>.

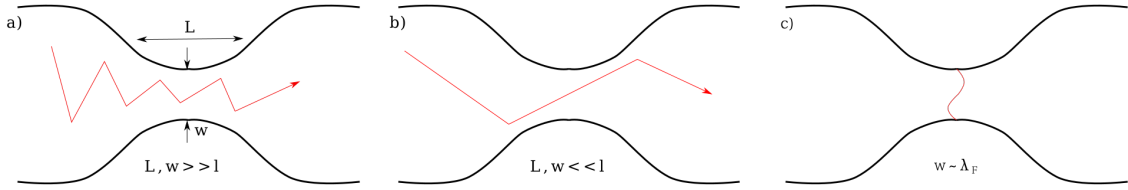


Figure 2.1: Schematic illustration of conductance in metallic contacts, a) diffusive, b) ballistic, c) quantum. Adapted from<sup>13</sup>.

When we are in the classical limit where  $l \ll w, L$  we are in the *diffusive* regime, Fig. 2.1 (a). In this regime, the electron travelling through the constriction will have a high probability to be scattered before it reaches the end of the constriction. In this regime the conductance was described by Maxwell and is given by

$$G = 2w\sigma. \quad (2.4)$$

As the constriction is shrinks until we reach the limit where  $l > L$  we reach to the *ballistic* regime, where the electron momentum can be assumed to be constant and is only scattered by the boundaries of the sample as shown in Fig. 2.1 (b). The conductance in this limit was described by Sharvin in 1965 and is given by

$$G = \frac{2e^2}{h} \left( \frac{k_F w}{2} \right)^2. \quad (2.5)$$

Sharvin found this expression by approximating the electrical current with the classical problem of dilute gas flow through an small hole. In this regime we can see the conductance  $G$  is proportional to the contact area like in the classical regime, but it has also a proportionality constant  $2e^2/h$  that has a quantum nature. In this regime we can see that the conductance is independent of the conductivity  $\sigma$  and the mean free path  $l$ <sup>14</sup>.

If we keep shrinking the constriction we will enter to the regime where contact width is of the order of a few nanometers or less, so we reach the point where the width of the contact is of the order of the Fermi wavelength,  $w \approx \lambda_F$ . At this point we enter to the *quantum* limit, Fig. 2.1 (c). The conductance at this limit will be quantized, the radial confinement will allow only a finite number of wavelengths to be

transmitted. By changing the size of the contact we could change the number of modes contributing to the conductance, changing the conductance in a step like manner. In this regime the electron scattering will occur mainly due the wall forming the boundary of the system<sup>1</sup>. This approach was derived by Rolf Landauer in the 1950s following the scattering approach. The basic idea of this approach is to relate the transport properties with the transmission and reflection probabilities for carriers incident in the sample as shown in Fig. 2.2. The main idea of this approach is to solve the Schrödinger equation, find the current eigenmodes, calculate their transmission probabilities and sum up their contributions. This idea is expressed by Landauer formula, shown below<sup>4 1</sup>.

$$G = \frac{2e^2}{h} \sum_{n=1}^N T_n, \quad (2.6)$$

where the summation is performed over all available conduction modes and  $T_n$  is their individual transmission coefficient with  $0 \leq T_n \leq 1$ . If we have a perfect transmission, each mode will contribute to one quantum unit of conductance,  $G_0 = 2e^2/h$  in a step like manner.

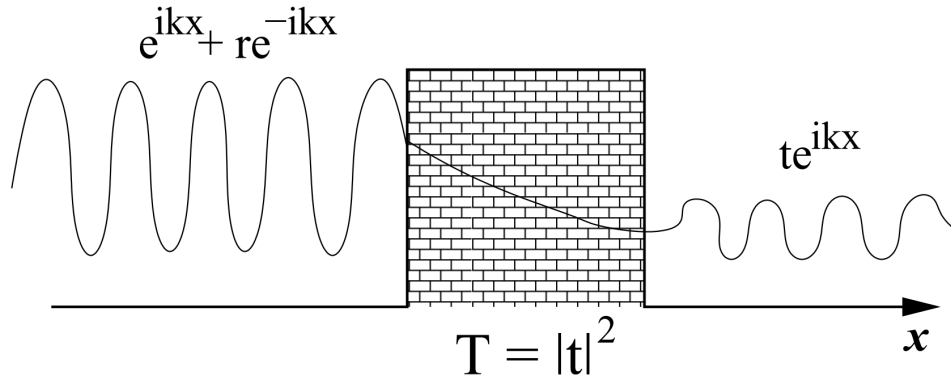


Figure 2.2: Wave function representation when impinging a potential barrier. The wave is partially reflected with an amplitude  $r$  and partially transmitted with and amplitude  $t$ . Retrieved from<sup>1</sup>.

### 2.1.1 Landauer formula heuristic derivation

When we perform a molecular junction experiment, our sample is connected to macroscopic electrodes that allow us to inject currents and fix voltages. These electrodes act as ideal electron reservoirs in thermal equilibrium with a well defined temperature and chemical potential. In the following section I will explain



an intuitive description to understand the relation between current and transmission. The current density is defined in the following way:

$$J_k = \frac{\hbar}{2m} i \left[ \psi^*(x) \frac{d\psi}{dx} - \psi(x) \frac{d\psi^*}{dx} \right] = \frac{e}{L} v(k) T(k), \quad (2.7)$$

where  $v(k)$  is the group velocity<sup>1</sup>. The group velocity can be derived by considering a free electron with energy

$$E = \frac{\hbar^2 k^2}{2m}. \quad (2.8)$$

We know that the momentum is related with the wave-number  $k$  by  $p = \hbar k$ . If we take the derivative of Equation 2.8 with respect to  $k$  and express this result in terms of momentum, we would obtain:

$$\frac{dE}{dk} = \frac{\hbar^2 k}{m} = \frac{\hbar p}{m}. \quad (2.9)$$

Then, by relating the momentum with velocity and by using previous results we would obtain<sup>16</sup>:

$$v = \frac{p}{m} = \frac{1}{\hbar} \frac{dE}{dk}. \quad (2.10)$$

By solving previous result we would obtain that the group velocity is<sup>16</sup>:

$$v(k) = \frac{\hbar k}{m}. \quad (2.11)$$

On the other hand, the current on a device occurs due to the movement of many electrons, therefore we introduce a sum over  $k$ . Since electrons are fermions we have to take into account also the Pauli exclusion principle, to do this we introduce the factor  $f_L(k) [1 - f_R(k)]$ , where  $f_{L,R}$  is the Fermi function of the electron reservoir on the left (L) and on the right (R) of the barrier. This factor ensures that current is produced only by the states that were initially occupied on the left and empty on the right. By taking into account all this, we would obtain that the current flowing from left to right is equal to:

$$J_{L \rightarrow R} = \frac{e}{L} \sum_k v(k) T(k) f_L(k) [1 - f_R(k)]. \quad (2.12)$$

To simplify the calculations of the current density we transform the summation to an integral by using the relation  $\frac{1}{L} \sum_k g(k) \rightarrow \frac{1}{2\pi} \int g(k)$  and obtain:

$$J_{L \rightarrow R} = \frac{e}{2\pi} \int dk v(k) T(k) f_L(k) [1 - f_R(k)]. \quad (2.13)$$

The next step is to perform a change of variables to express the current density in terms of energy instead of  $k$ . The change of variable will be done by using equation 2.9, which will give us:

$$\frac{dk}{dE} = \left( \frac{dE}{dk} \right)^{-1} = \frac{m}{\hbar^2 k}. \quad (2.14)$$

By replacing this results and results of the group velocity from equation 2.11 and simplifying terms we would obtain that current density from left to right is calculated with:

$$J_{L \rightarrow R} = \frac{e}{h} \int dE T(E) f_L(E) [1 - f_R(E)]. \quad (2.15)$$

In an analogous way the current density from right to left can be found to be:

$$J_{R \rightarrow L} = \frac{e}{h} \int dE T(E) f_R(E) [1 - f_L(E)]. \quad (2.16)$$

At the junction there will be a flow of electrons from left to right and a flow from right to left, so to calculate the the total current we need to find the difference between the current density from left to right and the current density from right to left.

$$I(V) = J_{L \rightarrow R} - J_{R \rightarrow L}. \quad (2.17)$$

Since we are performing all calculations in a  $1D$  situation, there is no difference between the total current and the current density. After doing some calculation we would obtain that the total current could be expressed as<sup>1</sup>:

$$I(V) = \frac{2e}{h} \int_{-\infty}^{\infty} dE T(E) [f_L(E) - f_R(E)]. \quad (2.18)$$

The factor of 2 appears to take into account the spin degeneracy. At very low temperature  $f_L(E)$  and  $f_R(E)$  are step functions equal to 1 between  $E_F - \frac{eV}{2}$  and  $E_F + \frac{eV}{2}$  and 0 outside of this energy range as shown in Fig. 2.3. Therefore by taking this approximation and by considering a perfect transmission ( $T = 1$ ), the total current can be approximated by:

$$I(V) = \frac{2e}{h} T \int_{E_F - \frac{eV}{2}}^{E_F + \frac{eV}{2}} dE. \quad (2.19)$$

$$I(V) = \frac{2e^2}{h} V. \quad (2.20)$$

By relating this result with equation 2.2 we can see the the conductance is equal to :

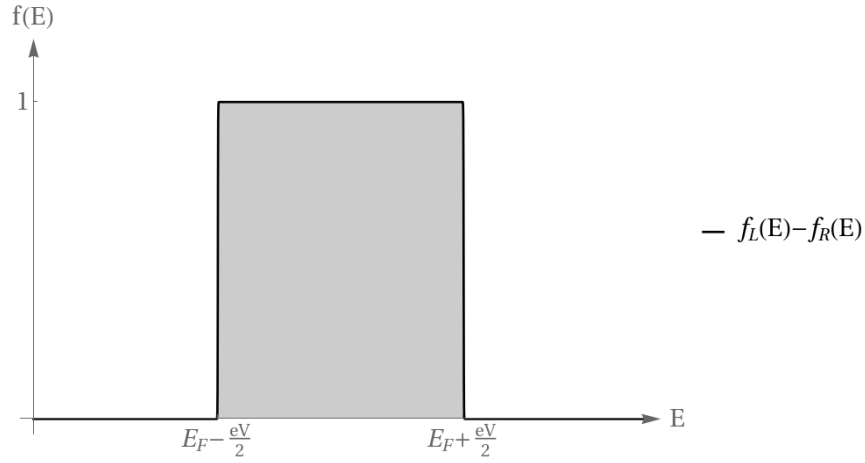


Figure 2.3: Graphical representation of  $f_L(E) - f_R(E)$  at low temperature.

$$G = \frac{2e^2}{h} = G_0. \quad (2.21)$$

$G_0$  is the conductance quantum unit that corresponds to 100% transmission of electrons from one electrode to the other through the point contact, which tells us how conductive is a molecule in comparison to the metal atom<sup>11</sup>. From this result we can observe that a perfect single mode conductor has a finite resistance equal to  $h/2e^2 \approx 12.9 \text{ k}\Omega$ . This result shows an important difference with macroscopic perfect conductors where one can expect to have zero resistance. This finite resistance could be arising from the interfaces between the lead and the sample<sup>14</sup>.

## 2.2 Solution to the simple problem for a quasi 1D metallic junction

The study of conduction through atomic scale wires started at the beginning of the 1990's. To have a better understanding of the conductance through molecular junctions, we need to understand some properties that occur at metallic contacts which are used as the electrodes in molecular junctions<sup>1</sup>. In bulk metals the electron wave function is confined in 3 spacial dimensions, resulting in a discrete set of energy level. If we shrink the bulk material until we reach the quantum limit the electron's wave function will be confined to 2 spatial dimension, creating a set of one dimension energy bands, referred as modes or channels<sup>17</sup>. In this limit, the main source of elastic scattering in these nano contacts are the walls at the boundary of the system<sup>1</sup>. In simple metals conductance is carried by a defined set of channels<sup>17</sup>, where the number of channels is expected to be small<sup>4</sup>. For a smooth and long wire the modes at the narrowest cross section

couple to a single mode at one of the sides of the contact, and the conductance expression shown in Eq. 2.6 could be simplified to<sup>17</sup>:

$$G = N_c G_0. \quad (2.22)$$

The number of conductance channels,  $N_c$ , can be calculated by:

$$N_c \approx \left( \frac{\pi r}{\lambda_F} \right)^2, \quad (2.23)$$

where  $r$  is the contact radius and  $\lambda_F$  is the Fermi wave length of the conduction electrons<sup>14</sup>. In metals  $\lambda_F \approx 5\text{\AA}$ <sup>4</sup> and the number of conductance channels lies between 1 and 3. The number of channels that contribute to the conductance depend on the geometry of the narrowest part of the contact and on the number of valence orbitals of the atom<sup>1</sup>. In some metals such as gold the conductance rises in steps of multiples of quantum unit of conductance, but this should not be expected to happen in every metal<sup>4</sup>.

For studying the conductance of atomic size contact the experimental techniques such as the MCBJ involve mechanically breaking and making cycles of a contact between two metal electrodes<sup>4</sup>. When we start pulling apart a metallic wire, one would expect that the conductance decreases smoothly, but experiments have shown that it decreases in a step wise manner in multiples of quantum units of conductance  $G_0$  as it can be seen in Fig. 2.4. For example in the case of gold the conductance measurements start with a reduction of the conductance periodically when the contact size is big but as the contact size reduces, conductance measurement start showing a series of plateaus that become more horizontal as the contact size is reduced and at the last plateau before loosing contact, conductance is almost flat and very close to  $1 G_0$ . It can also be observed that at the end of each plateau conductance decreases by a sharp jump that is of the order of one quantum unit,  $G_0$ <sup>41</sup> By doing a closer analysis of the conductance measurement of Fig. 2.4, it can be observed that many of the plateaus are not integer multiples of  $G_0$  and the structure of each step is different for each recording. It has been found that for metals the transition between plateaus is very sudden and sharp. These sudden jumps occur due to the sudden rearrangements of the contact. When the contact is stretched, there is an accumulation of elastic energy in the atomic bonds, this accumulation of energy is observed in the length of the plateau. Then this energy will be suddenly released in a transition to a new atomic configuration, resulting in a smaller contact size. This hypothesis was first proved experimentally by measuring the conductance and the force of the contact at the same time<sup>17</sup>. In Fig. 2.5 it can be observed the conductance results in a simulation of an Aluminium wire where it can be observed the atomic rearrangements as the coil is pulled apart with a reduction in the conductance. Each time when the contact is opened, and closed again to sufficiently large conductance values, random atomic reconfigurations take place, leading to a completely new set of scattering centers<sup>5</sup>.

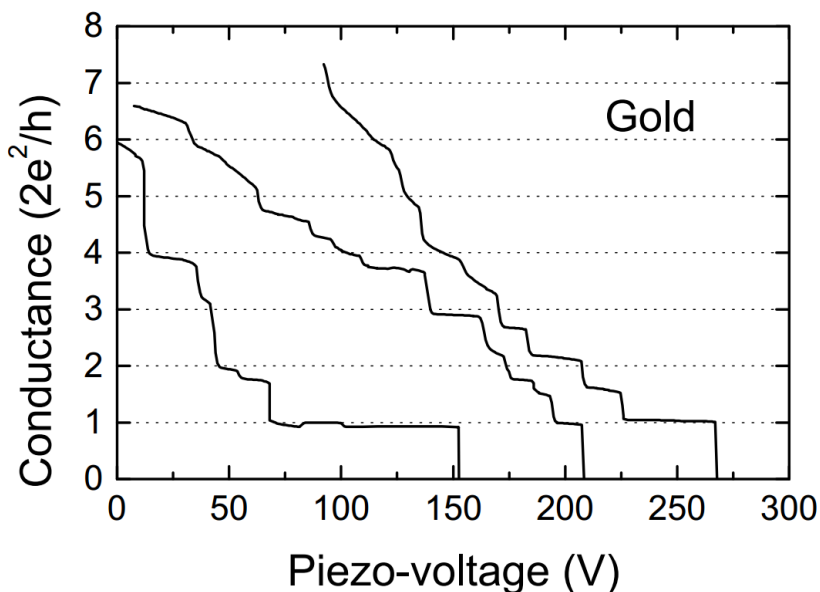


Figure 2.4: Recording of conductance  $G$  measured in atomic contacts for gold using MCBJ. Retrieved from<sup>1</sup>.

### 2.2.1 Conductance histograms

As it was mentioned previously and as it can be observed in Fig 2.4, the conductance of an atomic contact can be different in every measurement that is made, but there are certain features that are more probable to be repeated, like for example the last plateau in gold contacts. In order to solve this problem and to investigate conductance in atomic junction, scientists have developed a method which consist on recording histograms of of a large number of individual conductance vs. displacement curves<sup>41</sup>. This method exploits the variability in the data resulting from all the possible atomic contact configurations and assumes that all possible configurations have equal possibility to be formed. Under this assumption, it is expected to find the peaks in the histogram that correspond to conductance values that are preferred by the electronic system<sup>4</sup>, the height of the peak indicates which structures are the most stable<sup>3</sup>.

The histograms have the conductance measurements in the horizontal axis and counting of the measured conductance in the vertical axis, as can be seen in Fig. 2.6. The conductance axis is divided into a series of bins and the conductance values that fall within the range of each bin are collected from a large number of individual scans. The resolution of the measurements is limited by the width of each bin and also by the

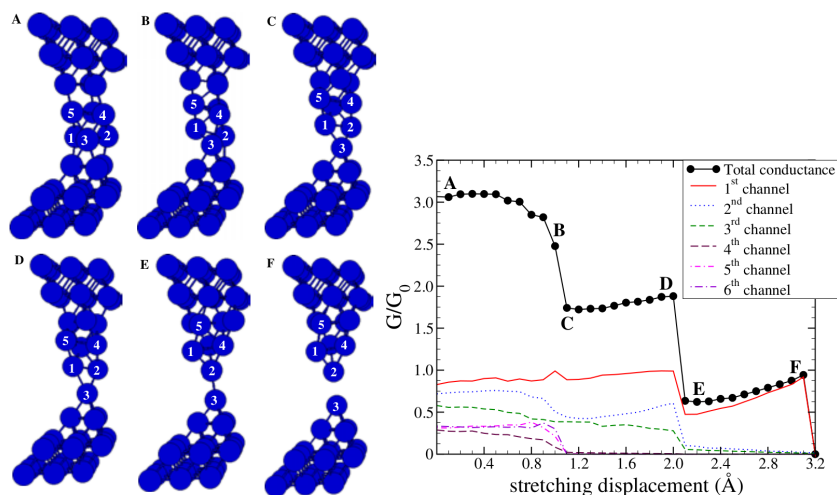


Figure 2.5: In the left picture it can be seen the evolution of the atomic rearrangements during the stretching of the wire. In the right picture it can be seen the conductance measurements and the channel contribution along the stretching path. Retrieved from<sup>1</sup>.

digital resolution of the analog-to-digital converter (ADC). To create an histogram we need thousands of conductance curves, for this reason the contact breaking is done in a very small time, around a second or shorter<sup>4</sup>, is important to mention that the lifetime of the contact increases as the stretching speed decreases<sup>3</sup>.

Not all metals show pronounced histogram peaks near integer conductance values. The most clear results where one can observe the quantization of conductance are obtained only for monovalent metals, such as the alkali metals like Li, Na and K; and also for the noble metals like Cu, Ag and Au<sup>1 17</sup>. The most studied metal has been gold, investigated with various techniques and under very different conditions. It has been found that many features in the histograms, recorded under very different conditions seem to reproduce. The reason for this to happen is due to the low reactivity of its surface and also because it is easily cleanable. As we can observe in Fig. 2.6 we can distinguish 3 peaks near 1, 1.8 and 2.9  $G_0$ . The first peak is very pronounced and much higher than the others and the others tend to decrease in height with a increasing conductance. It has also being found that the atmosphere does have an important effect in the measurements. By doing measurements at helium and rooms temperatures it has being found that there are not qualitative changes, the only change that can be found is the first peak increases its height by decreasing the temperature<sup>4</sup>. For all this reasons gold is the most common material used as electrodes in molecular junctions<sup>1</sup>.

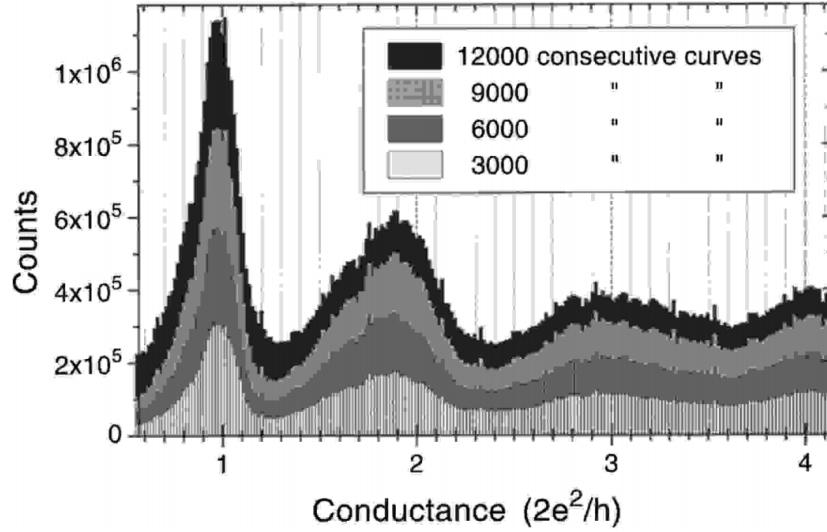


Figure 2.6: Gold conductance histogram. Retrieved from<sup>4</sup>.

## 2.3 Spin degree of freedom, ferromagnetic junctions

The use of the spin degree of freedom of the electron has led to the discovery of many fundamental effects and to new technological applications. In recent years there has been a lot of effort to understand how these fundamental effects are modified when the dimensions of a magnetic device are reduced to the atomic scale. Opposed to the level of understanding to the case of non-magnetic contacts, the physical understanding of ferromagnetic junctions is not well established and there are still basic open problems<sup>1</sup>.

### 2.3.1 Conductance on ferromagnetic atomic contacts

The interest in studying ferromagnetic metals came as a result of speculation that the strong exchange splitting of the electron bands may lift the spin degeneracy of conductance modes, which would give rise to half integer conductance steps,  $e^2/h$  instead of  $2e^2/h$ <sup>4</sup>. Studies of conductance in ferromagnetic materials like Fe, Co and Ni; have shown two types of contradictory results. Some studies have observed peaks in the conductance histograms at half-integer multiples of  $G_0$ . This results have been interpreted as a manifestation of half-integer conductance quantization, which implies that only fully open channels contribute to the conductance. In this sense, having a peak at  $0.5 G_0$  could also mean the existence of a fully polarized current. Experiments performed by Ludoph and Van Ruitenbeek<sup>5</sup> at a temperature of  $10 K$  have obtained a conductance peak at around  $2.2 G_0$  as it can be seen in Fig. 2.7 and Fig. 2.8. Another

group of experiments have found that the conductance histograms are featureless at room temperature as it can be seen in Fig 2.9<sup>18</sup>. An explanation for the difference of this results could be that in the room temperature experiments, contacts get contaminated by adsorbents from the atmosphere, which wash out the conductance features<sup>41</sup>. Another study performed by Ott *et al.*<sup>6</sup> has found very defined peaks at  $1G_0$ ,  $2G_0$  and  $3G_0$  as it can be observed in Fig. 2.10. This results may be due to the magnetization of the Fe wires<sup>64</sup>.

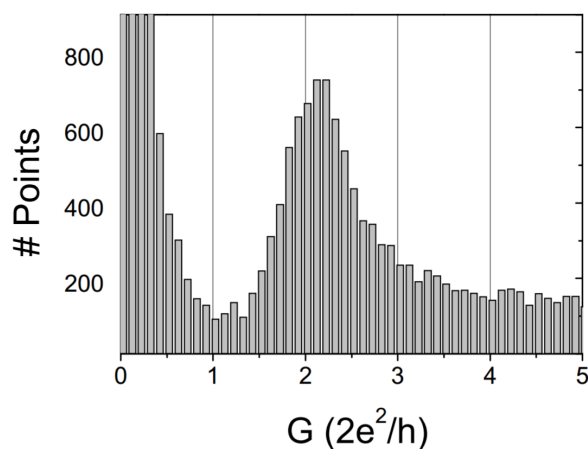


Figure 2.7: Iron conductance histogram measured at 10 K. Adapted from<sup>5</sup>.

From the wide variety of the results obtained in ferromagnetic materials, it was concluded that this material don't show consistent results, but there is evidence that the magnetization state and temperature modifies the conductance<sup>4</sup>. There have been also theoretical studies that suggest that transport in this kind of materials is not ballistic and conductance quantization should not be expected<sup>1</sup>

## 2.4 Molecular junctions

Research in the field of molecular junctions will make possible the use of molecules as possible building blocks in nanoscale circuits. Having a better understanding of the conductance in single molecules will allow us to have more control on the electronic transport, since metallic nanowires have a limited flexibility in many aspects. Some of the disadvantages of metallic nanowires are that is hard to change their conductance with a gate voltage and also their current-voltage characteristics are linear which limits the implementation of electronic functionalities. Molecules are still small enough to take advantage of their size and the great variety of the physical properties make them ideal to mimic ordinary microelectronics



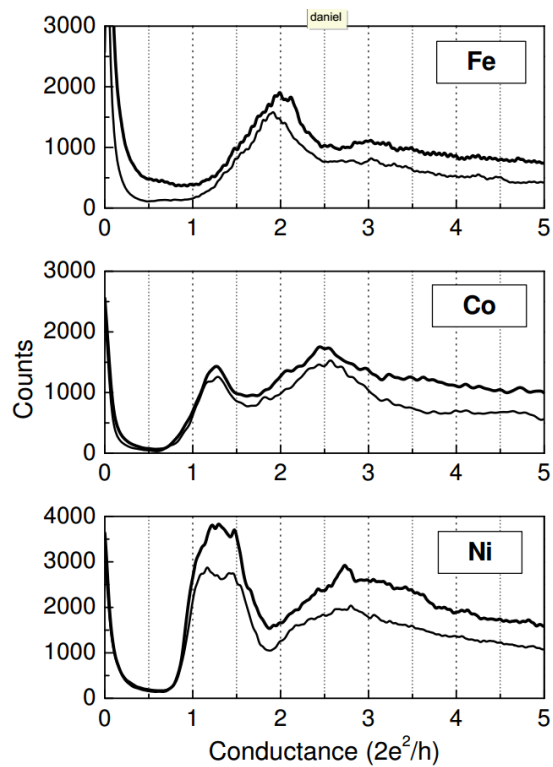


Figure 2.8: Conductance histograms for Fe, Co and Ni obtained by applying a magnetic field (thick curve) and without applying a magnetic field (thin curve). This measurement was performed at a temperature of 4.2 K. Retrieved from<sup>1</sup>.

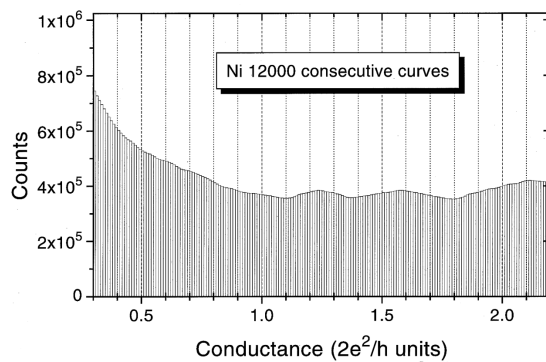


Figure 2.9: Iron conductance histogram measured at 10 K. Adapted from<sup>5</sup>.

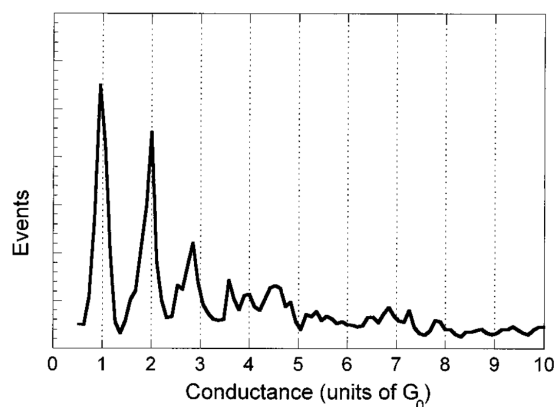


Figure 2.10: Iron conductance histogram measured with magnetically saturated wires. Retrieved from<sup>6</sup>.

components and also provide new electronic functions. Molecules offer this advantages, but there are still some problems that need to be solved on the experimental side, some of them are the reproducibility of the results, stability of the contacts, external control and mass production.

The theoretical description of conductance is more complicated than from atomic wires. From the theoretical point of view, for the description of molecular junctions we have to face four main challenges that could give molecules different functionalities. The challenges are the following.

1. Molecules have a more complicated electronic structure than an atom, because they are composed several atoms of different species.
2. At the junction with the electrodes, a molecule may have a weak chemical interaction, which may cause the the charge carriers spend a long time in the molecule.
3. Molecules posses internal degrees of freedom in particular vibrational modes, which can be excited by the transport electrodes leading to a modification of the current voltage characteristics.
4. Molecules can undergo conformational changes due to the high electric fields applied in the contacts, mechanical stress, external field or the local environment<sup>1</sup>.

### 2.4.1 Coherent transport through molecular junctions

Coherent transport through molecular wires is the regime in which the electrons flow elastically through the molecule without the exchange of energy<sup>1</sup>. According to Scheer and Cuevas<sup>1</sup> coherent transport is the regime in which the information about the phase of the wave-function of conduction electrons is preserved along the molecular bridges and the inelastic interactions take place only inside the electrodes, the molecule could be seen as the barrier from Fig 2.2 and the quantity that is measured is the transmission at the other electrode. A useful measurement that allow us to identify if the transport is coherent is the shape of the I-V curve and their temperature dependence. The four most studied conduction mechanisms are: direct tunneling, Fowler-Nordheim tunneling, thermionic emission and hopping conduction. This section will explain very briefly the most studied conduction mechanism in molecular junctions along with their dependence to voltage and temperature, which are summarized in Table 2.1.

Conducting mechanism	Characteristic behavior	Temperature dependence	Voltage dependence
Direct tunneling	$J \sim V \exp\left(-\frac{2d}{\hbar} \sqrt{2m\varphi_B}\right)$	None	$J \sim V$
Fowler-Nordheim tunneling	$J \sim V^2 \exp\left(-\frac{4d\sqrt{2m}\varphi_B^{3/2}}{3q\hbar V}\right)$	None	$\ln\left(\frac{J}{V^2}\right) \sim \frac{1}{V}$
Thermionic emission	$J \sim T^2 \exp\left(-\frac{\varphi_B - q\sqrt{qV/4\pi\epsilon d}}{k_B T}\right)$	$\ln\left(\frac{J}{T^2}\right) \sim \frac{1}{T}$	$\ln(J) \sim V^{1/2}$
Hopping conduction	$J \sim V \exp\left(-\frac{\varphi_B}{k_B T}\right)$	$\ln\left(\frac{J}{V}\right) \sim \frac{1}{T}$	$J \sim V$

Table 2.1: Molecular junction conduction mechanisms. Retrived from<sup>1</sup>.

Where the conduction mechanism are defined as:

- **Direct tunneling:** this process occurs when electrons go through a barrier when voltage is much smaller than the barrier height. In this process the I-V curves are insensitive to temperature.
- **Fowler-Nordheim tunneling:** the difference between this process and the previous one is that the voltage is larger than the barrier height. The other difference is their I-V curves has a different voltage dependence<sup>1</sup>. At certain voltage there could occur a transition from direct tunneling to this kind of mechanism<sup>19</sup>.
- **Thermionic emission:** this process occurs when the electrons are exited over a potential barrier,

as opposed to tunneling through it. As it can be seen in Table 2.1, this process has a very strong dependence on temperature, which can become very significant when the potential barrier is small.

- **Hopping conduction:** in this mechanism, electrons are localized at certain points within the molecule and can go between the points. This process has also a dependence on temperature. Conductance in most long molecules occur by this process, except in some special cases such as in carbon nanotubes.

If we want to separate the transport mechanism by their dependence in thermal activation, we could separate them in two categories: temperature-independent I-V characteristics such as in direct or Fowler-Nordheimer tunneling; and temperature dependent I-V characteristics such as in thermionic or hopping conduction. The transport regime can be characterized by the shape of I-V characteristic curves<sup>1</sup>.

### 2.4.2 Length dependence on the conductance

Length dependence is one of the most studied issues in molecular electronics. Series of molecules like alkanes, oligophenylenes, oligothiophenes, etc., have been extensively studied with different techniques. From all the studies the common result has been that conductance decays exponentially depending on the length of the molecule (L) following the equation below:

$$G(L) = A e^{-\beta L}, \quad (2.24)$$

where  $\beta$  is the attenuation factor<sup>1</sup> which describes the attenuation of current through the junction as a function of the distance (L) between the electrodes<sup>19</sup>. This factor depends on the type of molecule, the presence of side groups, on the bias voltage and on the anchoring groups. The factor  $A$  is just a prefactor that determines the order of magnitude of the conductance<sup>1</sup>. From experimental studies, many wired shaped molecules could be divided in two categories: saturated and conjugated chains.

#### Saturated chains

Saturated chains are small molecules with linkers at extremes to have a better connection with the electrodes, like for example alkanes. Some characteristics of this type of molecules are their large gaps between their Highest occupied molecular orbital (HOMO) and lowest unoccupied molecular orbital (LUMO) and their low conductivity. For example in alkanes it has been found that their conductance (G), decreases exponentially depending on their molecular length (L) and is described by the following equation:  $G = A e^{-\beta L}$ , where  $A$  is a constant and  $\beta$  is a decay constant that varies between  $\sim 0.7 - 0.9 \text{ \AA}^{-1}$ . The exponential

decay, the characteristics current voltage curves and its temperature independence suggest that conduction occurs due to electron tunneling.

### Conjugated chains

Since the tunneling conduction mechanism decreases really fast, there are other processes that occur for long distance charge transport. According to Tao<sup>2</sup> for long distance charge transport, conjugated molecule with alternating double and single bonds or with delocalized  $\pi$  electrons are better candidates. One important characteristic of this kind of molecules is that their HOMO and LUMO gap is much smaller which makes the charge transport more efficient. In this kind of molecules it is thought that conduction mechanism changes from a tunneling regime to a hopping regime. In the hopping conduction mechanism, charges hop from one site to the next along the molecule. This process can be activated thermally and has a weaker length dependence than in the tunneling process. Experiments have shown two characteristic behaviors in this process:

1. Charge transport can occur over a much greater distance.
2. There is a crossover from the tunneling regime to a hopping regime that occurs when the molecule's length is increased.

This kind of molecules have a smaller value of  $\beta$  which shows that conductance drops off slowly with chain length. For example, experimental measurements in carotenoid polyenes with different lengths have measured  $\beta = 0.22 \pm 0.04 \text{ \AA}^{-1}$ . The small value of  $\beta$  demonstrates that conductance drops at a slower rate with chain length. This unusual length-dependent conductance was attributed to the smaller gap between the HOMO and LUMO and to the closer position of the HOMO to the Fermi levels of the probing electrodes for the longer molecules<sup>2</sup>. A  $\beta$  value less than  $0.2 - 0.3 \text{ \AA}^{-1}$  is considered as an indication of hopping mechanism<sup>19</sup>.

## Chapter 3

# Experimental Methodology

### 3.1 State of the art of MCBJ

The MCBJ that is going to be used in this experiments was build by Werner Bramer, based on the equipment of Oren Tal's group at the Weismann Institute in Israel, which is one of the leaders in molecular electronics. This equipment is the first instrument of its kind completely built in Latin America. The electrodes that are going to be used are made from gold with an ultra-high purity of 99.999%. These metal wire was obtained with the collaboration from the University of Lorraine, France. The metal wire can be seen in Fig. 3.1.



Figure 3.1: Gold metal wire for the construction of the electrodes with an ultra-high purity of 99.999%.

The MCBJ system could be divided into two categories: the break junction and the fast electronics setup to acquire the data. The break junction is composed of the main head (Fig. 3.2), the sample holder

(Fig. 3.12), the main head mounting, the micro-metric screw, the low frequency canceling tube and the cover of the main head, which can be seen in Fig 3.3. The main head has the piezoelectric glued to a mobile base to adjust its height to the sample, which is held in place by the sample holder. The mobile base movement is controlled with the micro-metric screw. The main head is covered to prevent any dust from entering the sample causing noise in the measurements. All this setup is placed on top of a rubber tube to cancel low frequency vibrations that may cause noise in the measurements.

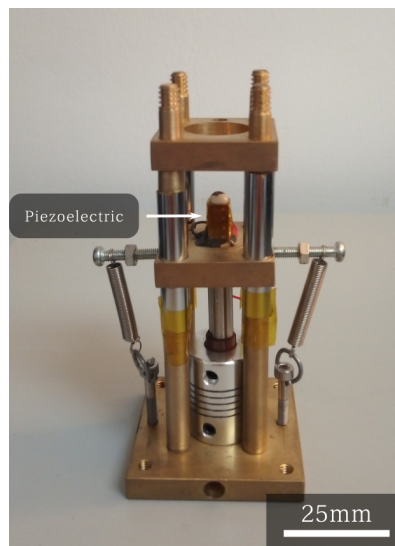


Figure 3.2: MCBJ main head.

The fast electronics setup is composed of the bias voltage controller, the piezo controller, a preamplifier, the oscilloscope, the data acquisition (DAQ) and the computer, which can be observed in Fig 3.4 and Fig. 3.5. The piezo controller controls the up and down movement of the piezoelectric for breaking the gold wire. Then we have a preamplifier that amplifies the signal so it can be observed in the oscilloscope or read by the DAQ. The sample could be connected to the oscilloscope to observe the breaking measurements live. Then the other component is the DAQ that allows to make the readings and transfer them to the computer. The daq manufacturer is Measurement Computing, model *USB-1808X*, which has a resolution of 18 bits and a max sample rate of 200 *KS/s*. Finally we have the computer, which is connected to the DAQ allowing us to save the measurements and to the piezo controller. The complete setup of the system can be observed in Fig. 3.6

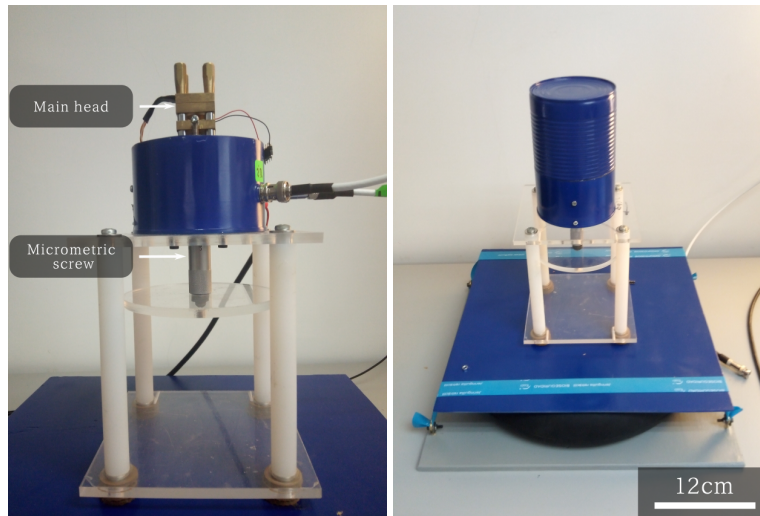


Figure 3.3: Fully assembled MCBJ.

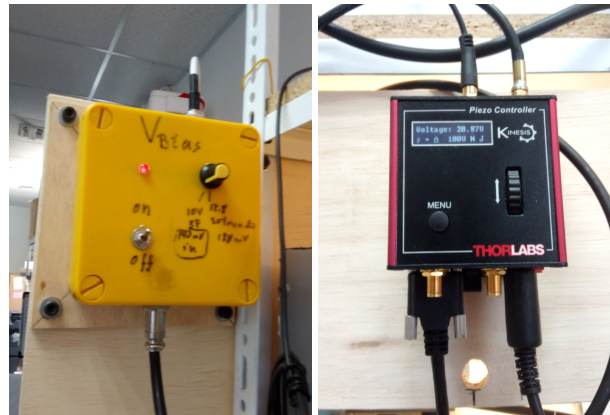
Figure 3.4: Fast electronics equipment. Left: bias voltage ( $V_{bias}$ ) controller, in this experiment is set to  $100mV$ . Right: piezocontroller from Thorlabs, used for up and down movement of the piezoelectric.





Figure 3.5: Fast electronics equipment. Left: Oscilloscope. Center: I/V preamplifier, in this experiment for metallic junction amplifies the signal  $10^5$  and for molecules  $10^6$ . Right: DAQ from Measurement Computing, model USB-1808X, with a resolution of 18 bits and a max sample rate of 200 *KS/s*.

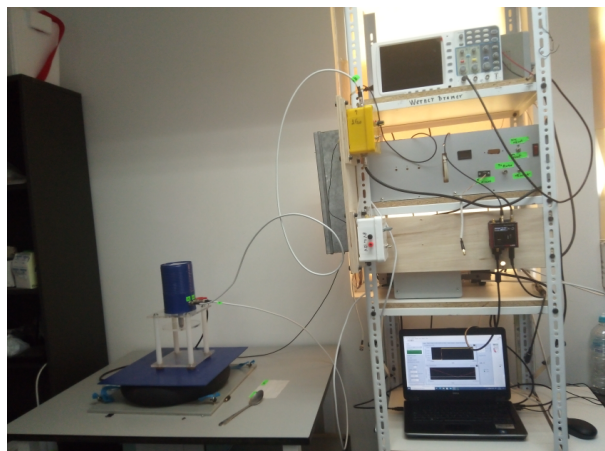


Figure 3.6: Complete MCBJ equipment.

In order to build the electrodes it is necessary to make a superficial cut in the wires to reduce the width of the wire to 1/3 of its original width. To achieve this we used a device to make precise cuts without completely cutting the wire that is shown in Fig. 3.7. Another important tool for the process of building the electrodes and preparing the sample is the stereoscopic magnifier, which is shown in Fig. 3.7

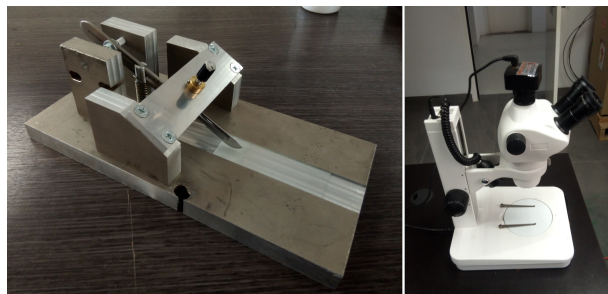


Figure 3.7: Left: wire slicing device to make a groove with a diameter of 1/3 of the original width of the wire. Right: stereoscopic magnifier.

### 3.2 Mechanics and electronics of the MCBJ

To be able to make the measurements the break junction system is connected in the following way. The first connection is the piezo controller to the computer and the piezo controller to the piezoelectric. This connection controls the up and down movement of the piezoelectric to break and join the gold wire. The parameters sent to the piezocontroller are voltage between 0 and 70 Volts with a delay of 150ms, this parameters are set in the program shown in Fig. 3.9. Then the bias voltage ( $V_{bias}$ ) is connected to the gold junction, in this experiment the  $V_{bias}$  is set to 100mV. The  $V_{bias}$  out of the junction goes to a preamplifier, for metallic junctions is set to amplify the signal to  $10^5$  and for measuring molecules is set to  $10^6$ . After the signal goes through the preamplifier, the signal is processed in the DAQ. Finally, the signals are sent into a computer where they are saved and processed. To process and save the measurements we use the program built in LabVIEW, shown in Fig. 3.9. In case the readings need to be observed live, the signal going out the preamplifier can be connected to an oscilloscope. The circuit diagram of the connection can be seen in Fig. 3.8.

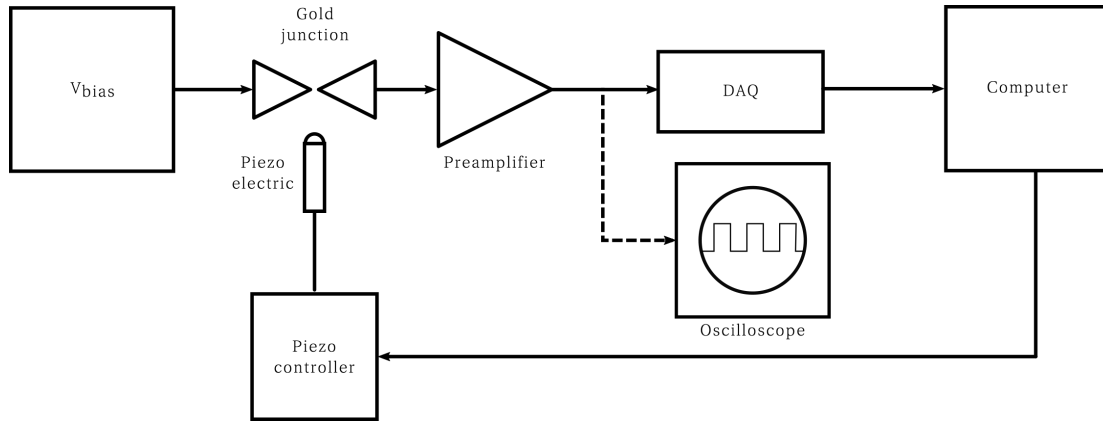


Figure 3.8: Circuit diagram with the components and the connection of the MCBJ.

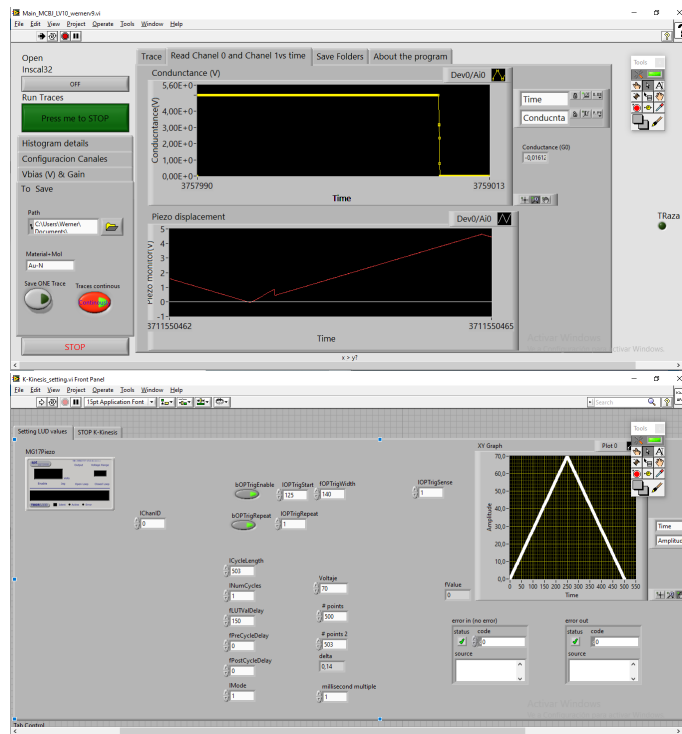


Figure 3.9: Program built in LabVIEW by Werner Bramer and Carlos Sabater for making the measurements. Top: program used to save the traces measured in the MCBJ. Bottom: program that controls the up and down movement of the piezoelectric.

### 3.3 Conductance measurements

#### 3.3.1 Sample preparation

The sample to make the measurements is prepared by doing the following process. The first step, is to place the gold wire between two microscope slides and move the slides back and forth for straightening the wire so it can roll when is placed in the wire slicing device. The second step is to place the wire on another slide on the wire slicing device, and move the slide toward the knife to create the groove on the wire. To have a good quality groove we first need to calibrate the wire slicing device by moving the knife down in very small steps. When the wire is ready it had to cleaned by using a piranha solution, in a 3 : 1 ratio of hydrogen peroxide and sulfuric acid, respectively. The wire is placed into this for 5 minutes, then it was washed with destiled water and the sample was dried with Argon gas. The next step was to prepare the copper substrate with Kapton tape and fix the wire using two drops of nail polish at the edges of the wire. The next step was to place two drops of the epoxy adhesive at each side of the groove and guide them until they are over the groove in a triangular shape, as can be seen in Fig. 3.11. When the adhesives were already dry, the substrate was placed in the sample holder and the gold wires were connected using silver paste, as can be seen in Fig. 3.12. The last two steps had to be done using the stereoscopic magnifier. In Fig. 3.10 there is a scheme of the process of the sample preparation. The epoxy adhesive is important that hold the gold wire very well to the substrate and does not break when the piezoelectric deforms the substrate. Placing the epoxy adhesive is a very important part of sample preparation and has to be done very carefully following a three step process.

1. Prepare the mixture of the two parts epoxy adhesive with a 1 : 1 ratio.
2. Let the adhesive dry for 3 minutes and then place 2 drops near the constriction site.
3. Let the adhesive dry for another 3 minutes and start driving the adhesive to toward the constriction site by giving them a triangular shape, as shown in Fig. 3.11.

#### 3.4 Measurement of the resolution of the MCBJ

The measurement of the resolution is important because it will let us know what kind of molecules the equipment is going to be able to measure. This measurement tells us the amount of electrical and environmental noise the equipment is detecting. To make the measurement we need to completely break the junction and collect measurements with an open circuit. Then we have to analyze and build an histogram

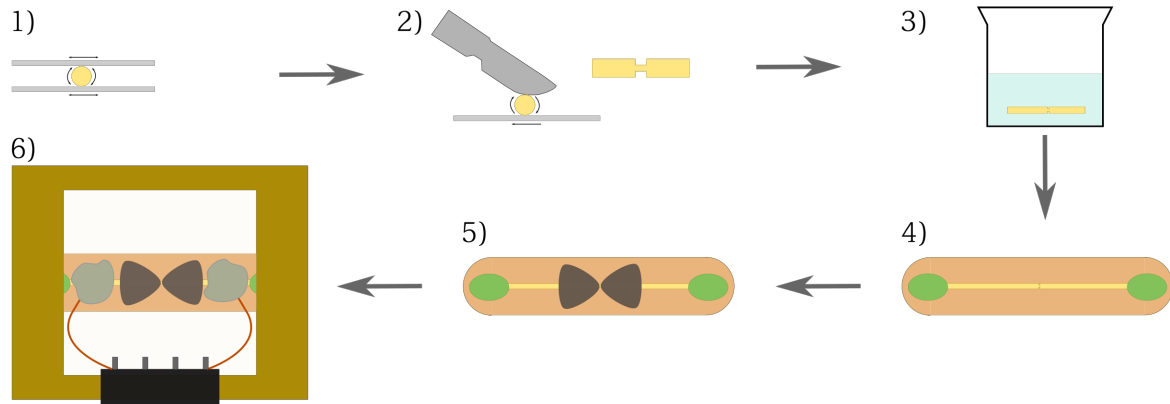


Figure 3.10: Sample preparation process. 1) Straightening of the wire between two microscope slides. 2) Creation of the groove in the wire using the device shown in Fig. 3.7. 3) Grooved wire in the piranha solution. 4) Fixing the gold wire on the substrate covered with Kapton tape with nail polish. 5) Placing two drops of epoxy adhesive at each side of the groove with a triangular shape. 6) Placing the substrate in the sample holder and making the connections using silver paste. Steps 5) and 6) are performed under the stereoscopic magnifier.

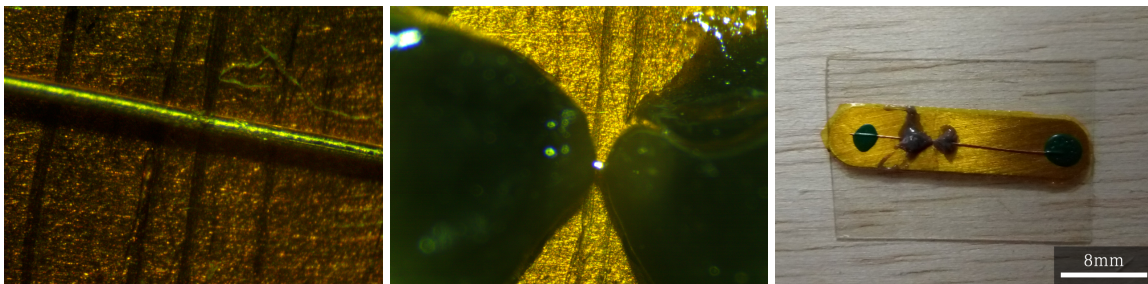


Figure 3.11: Sample preparation. Left: gold wire with the groove. Center: gold wire with the epoxy adhesive in triangular shape. Right: substrate ready to be placed in the sample holder.

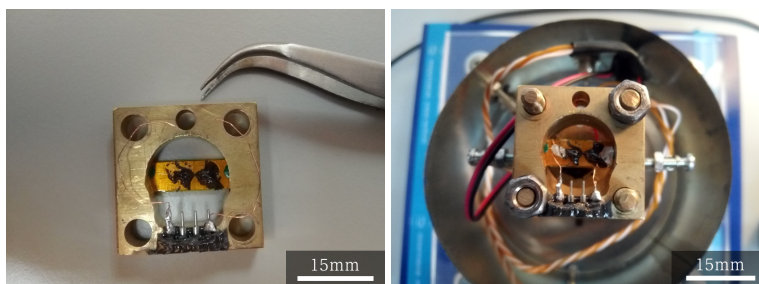


Figure 3.12: Left: sample ready. Right: sample placed in the MCBJ.

with this data, as shown in Fig. 3.13. It can be observed that the resolution of the equipment has an average of  $0 G_0$  with a standard deviation of  $0.001 G_0$ , and a maximum and minimum value of  $-0.003 G_0$  and  $0.003 G_0$  respectively. The average resolution of the equipment is  $0 G_0$ , because when there is nothing connected to equipment, there is an electrical noise coming from the environment and the connections on the equipment, that oscillates around  $0 G_0$ . Having the average resolution at  $0 G_0$ , shows this oscillation is occurring with the same amount of points below and above  $0 G_0$ . This also indicates that the equipment is well calibrated and that the measurements with the gold wire connected will be the correct ones. With the measurements of the resolution a good candidate that could be used to measure its conductivity would be the molecule of *benzene*, which has a high enough conductance to be detected by the MCBJ.

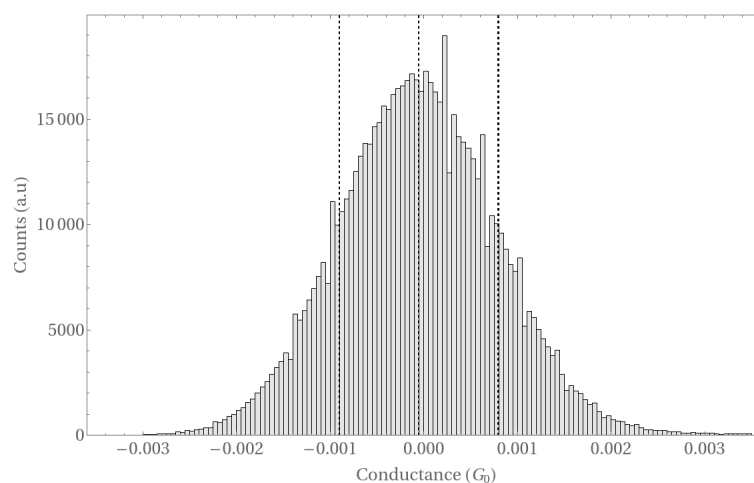


Figure 3.13: Resolution of the MCBJ.

### 3.5 Proposed experimental developments

In order to make the measurements of a metallic junction, the sample is placed in the MCBJ as seen in Fig. 3.12, make all the connections and run the programs shown in Fig. 3.9. To be able to obtain a good quality histogram it is needed to obtain around  $\sim 2000$  traces. Then all the collected traces are processed using a program built in *Mathematica* to create the conductance histogram of a metallic junction. All the measurements are performed at ambient conditions.

The first measurement that was performed was the measurement of a clean gold junction by amplifying the output signal from the junction with the I/V preamplifier  $10^5$  times, this measurement was performed to make sure that the equipment is working well and that we have the correct gold conductance measurements. Next, it was measured the conductance of a clean gold junction, but this time the output signal was amplified  $10^6$  times, this measurement will be the reference measurement to be able observe the effect the benzene produces in the conductance measurements. Since the measurement of a conductance molecule is way below  $1G_0$ , the signal needs to be amplified  $10^6$  times to be able to distinguish the conductance of a molecule. The last measurement was of *benzene* molecules, which according to de Ara *et al.*<sup>7</sup> has a high enough conductance to be measured by the equipment with its current resolution. The conductance measurement of a benzene molecule was done by placing a drop from a dropper of around  $30\mu\text{l}$  of a benzene solution in the junction.

### 3.6 Reference molecules measurement expectations

According to de Ara *et al.*<sup>7</sup> we could expect that the benzene molecules will affect the conductance in the following ways. From the research performed at the University of Alicante, one effect that benzene will cause is that the main gold peak in the histogram will be shifted to the right with respect to the clean gold peak and will also cause that the main peak becomes narrower. Regarding the conductance of a benzene molecule it can be expected that we have a really small peak at around  $\sim 0.18G_0$ . Then after applying the logarithm to the conductance values to observe with more clarity the low conductance values it can be expected to observe peaks at  $-0.768 \text{Log}(G/G_0)$  and at  $-1.98 \text{Log}(G/G_0)$ . The observation of peaks at lower positions will be harder since the resolution of the equipment doesn't allow us.

	<b>Main peak</b>	<b>Benzene peak</b>	<i>Log(G/G<sub>0</sub>)</i>
Gold	0.961	–	–
Gold-Benzene	0.973G <sub>0</sub>	0.18G <sub>0</sub>	–0.768 and –1.98

Table 3.1: Expected conductance benzene molecules de Ara *et al.*<sup>7</sup>.





# Chapter 4

## Results & Discussion

### 4.1 Tight binding model

In molecular electronics we want to establish a relationship between the transport properties of a molecular junction and their corresponding electronic structure of their isolated molecule. This section was done in collaboration with Ismael Villegas and Jonathan Pineda as part of the course of Solid state physics 2. The tight binding approximation is an approach to calculate electronic band structures by overlapping a set of wave functions of isolated atoms<sup>20</sup>. This model allows predicting the properties of systems composed of collection of atoms located at different positions. From this approach the Hamiltonian is build as a linear combination of atomic orbitals (LCAO), and can be obtained as an approximation of the Schrödinger equation written in terms of the continuous coordinate  $x$ .

$$-\frac{\hbar^2}{2m}\nabla^2\psi(x) + U(x)\psi(x) = \varepsilon\psi(x). \quad (4.1)$$

Which after a discretization of the Laplacian can be expressed as:

$$-\frac{\hbar^2}{2m}\frac{\frac{\psi(x+\Delta x) - \psi(x)}{\Delta x} - \frac{\psi(x) - \psi(x-\Delta x)}{\Delta x}}{\Delta x} + U(x)\psi(x) = \varepsilon\psi(x). \quad (4.2)$$

Then, defining  $x = na$  which could be interpreted as the position at one site and  $\Delta x = a$ , which could be interpreted as the distance between each site; would give us:

$$-\frac{\hbar^2}{2m}\frac{\psi(na+a) + \psi(na-a) - 2\psi(na)}{a^2} + U(na)\psi(na) = \varepsilon\psi(na). \quad (4.3)$$

Now defining  $\psi(na) = U_n$ ,  $V = \frac{\hbar^2}{2ma^2}$  and  $\varepsilon_n = U(na) - 2V$ , we would obtain:

$$\varepsilon_n U_n - V U_{n+1} - V U_{n-1} = E U_n^{21}. \quad (4.4)$$

## 4.1.1 Cyclic molecule: benzene

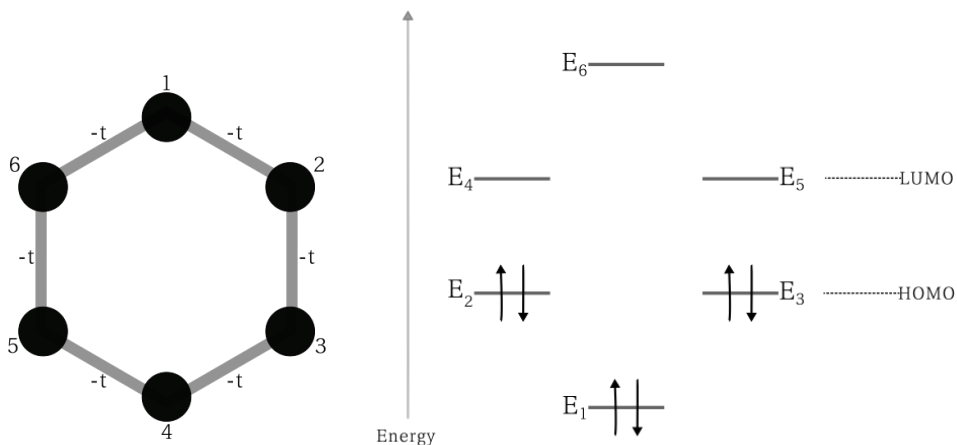


Figure 4.1: Left: scheme of a benzene molecule used to calculate the electronic structure using simple tight binding model. Right: energy levels diagram of benzene, obtained using this approximation; we have a HOMO-LUMO gap equal to  $2t$  and a total energy  $E_T = 6\epsilon_0 - 8t$ . Adapted from<sup>1</sup>.

Benzene is an example of a molecule in which its electronic structure is determined by the conjugated  $\pi$  system. This means that electrons in the highest occupied orbitals are located in the  $\pi$  orbitals formed by the  $2p_z$  orbitals (perpendicular to the plane of the molecule). Having a conjugated system allows the molecule to gain stability or binding energy by delocalizing the electrons over several neighboring atoms<sup>1</sup>. By using Eqn. 4.4 to write the tight binding model for benzene we would obtain the Hamiltonian

$$H = \begin{pmatrix} \epsilon_1 & -V_{1,2} & 0 & 0 & 0 & -V_{1,6} \\ -V_{2,1} & \epsilon_2 & -V_{2,3} & 0 & 0 & 0 \\ 0 & -V_{3,2} & \epsilon_3 & -V_{3,4} & 0 & 0 \\ 0 & 0 & -V_{4,3} & \epsilon_4 & -V_{4,5} & 0 \\ 0 & 0 & 0 & -V_{5,6} & \epsilon_5 & -V_{5,6} \\ -V_{6,1} & 0 & 0 & 0 & -V_{6,5} & \epsilon_6 \end{pmatrix}. \quad (4.5)$$

Then by using *Hückel* approximation, which is based on the following four basic assumptions, the Hamiltonian can be simplified. The first, is that only  $\pi$  orbitals are considered, which in the case of benzene, only one orbital per carbon atom will be taken into account. The second, the overlap integrals between different orbitals will be set to zero:  $S_{ij} = \delta_{ij}$ . Third, all the diagonal elements of the Hamiltonian

are written with the same value:  $H_{ii} = \varepsilon_0$ . Lastly, the off-diagonal elements are set to zero, except for those between neighboring atoms, which will be set to  $t$ , where  $t$  is positive<sup>1</sup>. Resulting in following Schrödinger equation

$$\begin{pmatrix} \varepsilon_0 & -t & 0 & 0 & 0 & -t \\ -t & \varepsilon_0 & -t & 0 & 0 & 0 \\ 0 & -t & \varepsilon_0 & -t & 0 & 0 \\ 0 & 0 & -t & \varepsilon_0 & -t & 0 \\ 0 & 0 & 0 & -t & \varepsilon_0 & -t \\ -t & 0 & 0 & 0 & -t & \varepsilon_0 \end{pmatrix} \cdot \begin{pmatrix} U_1 \\ U_2 \\ U_3 \\ U_4 \\ U_5 \\ U_6 \end{pmatrix} = E \begin{pmatrix} U_1 \\ U_2 \\ U_3 \\ U_4 \\ U_5 \\ U_6 \end{pmatrix}. \quad (4.6)$$

From the Schrödinger equation we know that

$$\begin{aligned} H\psi &= E\psi. \\ (H - E)\psi &= 0. \end{aligned}$$

For this system to have a valid solution and obtain the energies on each state we have to solve the eigenvalue equation

$$\begin{aligned} \text{Det}(H - E) &= 0. \\ \begin{vmatrix} \varepsilon_0 - E & -t & 0 & 0 & 0 & -t \\ -t & \varepsilon_0 - E & -t & 0 & 0 & 0 \\ 0 & -t & \varepsilon_0 - E & -t & 0 & 0 \\ 0 & 0 & -t & \varepsilon_0 - E & -t & 0 \\ 0 & 0 & 0 & -t & \varepsilon_0 - E & -t \\ -t & 0 & 0 & 0 & -t & \varepsilon_0 - E \end{vmatrix} &= 0. \end{aligned}$$

By solving the characteristic equation we obtain the following eigenenergies:

$$\begin{aligned} E_1 &= \varepsilon_0 - 2t, \\ E_2 &= E_3 = \varepsilon_0 - t, \\ E_4 &= E_5 = \varepsilon_0 + t, \\ E_6 &= \varepsilon_0 + 2t. \end{aligned}$$

The calculations of the eigenfunction are done by taking advantage of the symmetry of the molecule, simplifying the calculations. The calculations of benzene which has a  $6 \times 6$  determinant, are simplified

by taking advantage of the  $D_{6h}$  symmetry, but since every  $2p_z$  - orbital changes sign under a reflection in the molecular plane we could simplify more the calculations by using the  $C_{6v}$  symmetry. The calculation involve setting the carbon atoms as peripheral atoms of the molecule and setting up symmetry-adapted linear combinations (SALC) of the  $2p_z$  - orbital<sup>22</sup>, resulting in the following eigenfunctions:

$$\begin{aligned}\psi_1 &= \frac{1}{\sqrt{6}} (|1\rangle + |2\rangle + |3\rangle + |4\rangle + |5\rangle + |6\rangle), \\ \psi_2 &= \frac{1}{\sqrt{12}} (2|1\rangle + |2\rangle - |3\rangle - 2|4\rangle - |5\rangle + |6\rangle), \\ \psi_3 &= \frac{1}{2} (|2\rangle + |3\rangle - |5\rangle - |6\rangle) \\ \psi_4 &= \frac{1}{\sqrt{12}} (2|1\rangle - |2\rangle - |3\rangle + 2|4\rangle - |5\rangle - |6\rangle), \\ \psi_5 &= \frac{1}{2} (|2\rangle - |3\rangle + |5\rangle - |6\rangle), \\ \psi_6 &= \frac{1}{\sqrt{6}} (|1\rangle - |2\rangle + |3\rangle - |4\rangle + |5\rangle - |6\rangle)^{122}.\end{aligned}$$

As it can be observed in Fig. 4.1 (left), at the ground state the three lower states are occupied by the six  $\pi$  electrons. It can also be observed that the second and third as well as the fourth and fifth levels are degenerated. The total energy of benzene molecule is equal to  $E_T = 6\varepsilon_0 + 8t$ . It can also be observed that the HOMO-LUMO gap is equal to  $2t$ . As it was mentioned previously, the delocalization or conjugation of  $\pi$  electrons increases the stability or the binding energy of the molecule . In benzene if the electron were not conjugated the total energy of the molecule would be  $6(\varepsilon_0 - t)$ , but since there is conjugation occurs there is an increase in the energy of the molecule of  $-2t$  which is called delocalization energy<sup>1</sup>.

#### 4.1.2 Transmission of a benzene molecule

To calculate the electron's transmission of a benzene molecule it is needed to define a new Hamiltonian with electrodes attached to different sites of the molecule. The electrodes can be modeled as a semi-infinte chain of atoms that could be represented as:

$$\Sigma = \Delta \pm i\Gamma, \quad (4.7)$$

where  $\Delta$  and  $\Gamma$  are defined as:

$$\Delta = \frac{\varepsilon - E_{r0}}{2}. \quad (4.8)$$

$$\Gamma = \begin{cases} 0 & \text{if } |\varepsilon - E_{r0}| > 2|t_r| \\ \sqrt{\left(t_r^2 - \frac{\varepsilon - E_{r0}}{2}\right)^2} & \text{if } |\varepsilon - E_{r0}| \leq 2|t_r| \end{cases}, \quad (4.9)$$

where  $t_r$  is the coupling between gold atoms and  $E_{r0}$  is the onsite energy for gold atoms. For a transmission of electrons to occur the energy of the electrons should be within the range of the density of states (DOS) of the infinite chain of atoms, which is defined as:

$$N_r = \frac{1}{\pi t_r} \sqrt{1 - \left(\frac{\varepsilon - E_{r0}}{2t_r}\right)^2}. \quad (4.10)$$

It has been found that there is a relationship between the electron transmission and the contact geometry between the electrodes and the benzene molecule<sup>23</sup>. This section is going to show the differences in transmission when there is a parallel and perpendicular coupling of a benzene molecule between two semi-infinite chain electrodes. When there is a parallel coupling of the molecule we could have an *ortho* (sites 1 – 2), *meta* (sites 1 – 3) and *para* (sites 1 – 4) configurations, as shown in Fig 4.2.

To calculate the transmittance it is needed to calculate the Green's functions. The Green's function provide an alternative framework to discuss the solutions to the Schroödinger equation. With the Hamiltonian of the benzene molecule defined in Eqn. 4.6, we are able to calculate the Retarded (R) and Advanced (A) Green's functions and with this results we are able to calculate the transmittance of a benzene molecule<sup>21</sup>.

$$G^R(\varepsilon) = [(\varepsilon + i\eta)\mathbf{I} - \mathbf{H}]^{-1}. \quad (4.11)$$

$$G^A(\varepsilon) = [(\varepsilon - i\eta)\mathbf{I} - \mathbf{H}^*]^{-1}. \quad (4.12)$$

Then after calculating the advanced and retarded Green's function we are able to calculate the transmittance of a benzene molecule when it is coupled to electrodes in terms of the energy. The transmittance through a molecule is calculated by using the following equation:

$$T_{\alpha R, \beta L} = 2^\alpha \Gamma_R(\varepsilon) G_{\alpha R, \beta L}^R(\varepsilon) 2^\beta \Gamma_L(\varepsilon) G_{\beta L, \alpha R}^A(\varepsilon)^{21}. \quad (4.13)$$

To have a transmittance that makes sense with a value between 0 and 1 in an interval of energy, we need to normalize the transmittance  $T_{\alpha R, \beta L}$  by using the equation below. The multiplication by density of states  $N_r$ , is done because to have a transmittance there needs to exist non-zero states in the semi-infinite chain.

$$T_{Normalized} = T_{\alpha R, \beta L} \times N_r \times \left( \int_{-\infty}^{+\infty} T_{\alpha R, \beta L} \times N_r dE \right)^{-1}. \quad (4.14)$$

To calculate the coupling between the atoms we can use the following equation:

$$t_{ll'm} = \eta_{ll'm} \frac{\hbar^2}{md^2}, \quad (4.15)$$

where  $m$  is the mass of the electron,  $d$  is the distance between atoms,  $\hbar$  is the value of the reduced plank constant,  $\eta$  is a constant related to the orbital shape such as  $pp\pi$ ,  $ss\sigma$  or  $sp\sigma$ <sup>24</sup>. In the case of a benzene molecule, according to Harrison<sup>24</sup> and Hinkle<sup>25</sup> for the  $p_z$  orbitals the on site energy is equal to  $\varepsilon_0 = -8.97 \text{ eV}$ , the shape of the orbitals is  $pp\pi$  so  $\eta_{pp\pi} = 3.24$  and the distance between carbon atoms is equal to  $1.24 \text{ \AA}$ . By replacing this values in Eqn. 4.15 we would obtain  $t = -4.01 \text{ eV}$ . Then by replacing the on site energy  $\varepsilon$  and the coupling between carbon atoms on the calculated eigenenergies, we would obtain the following eigenenergies<sup>25</sup>:

$$\begin{aligned} E_1 &= -16.99 \text{ eV}, \\ E_2 &= E_3 = -12.98 \text{ eV}, \\ E_4 &= E_5 = -4.96 \text{ eV}, \\ E_6 &= -0.95 \text{ eV}. \end{aligned}$$

When the benzene is coupled to the gold electrodes it can be coupled in two configurations, parallel as shown in Fig. 4.2 or perpendicular<sup>7</sup>.

### Parallel coupling

In the parallel coupling the benzene could be coupled in three different configurations: *para*, when coupling is between sites 1 and 4; *meta*, when coupling is between sites 1 and 3; and *ortho*, when coupling is between sites 1 and 2;<sup>23</sup> as shown in Fig. 4.2. To calculate the transmittance it is first needed to define a new Hamiltonian adding the terms related to the gold chain ( $\Sigma$ ) and the coupling between the gold atoms and the benzene molecule. As shown in Eqn. 4.16, where  $t_s$  is coupling between gold and carbon atoms. The value of  $t_r$  is calculated using Eqn. 4.15, where the distance between gold atoms is  $d = 2.88 \text{ \AA}$ <sup>26</sup> and the orbital shape is  $ss\sigma$ , so the constant  $\eta_{ss\sigma} = -1.4$ <sup>24</sup>. Using this parameters we would obtain that the value of  $t_r = -1.28 \text{ eV}$ . In the same way for  $t_s$ , the distance between gold and carbon atoms is set to  $d = 6.5 \text{ \AA}$  and since the orbital shape is  $sp\sigma$ ,  $\eta_{sp\sigma} = 1.84$ <sup>24</sup>. With this parameters the value of  $t_s$  results in  $t_s = 0.33 \text{ eV}$ . For gold according to Harrison<sup>24</sup>, the on site energy is equal to  $E_{r0} = -6.48 \text{ eV}$ .

With this parameters set we can define a new Hamiltonian to calculate the transmission when the gold electrodes are attached in *para* configuration by adding the semi-infinite gold chain terms on sites 1 and 4

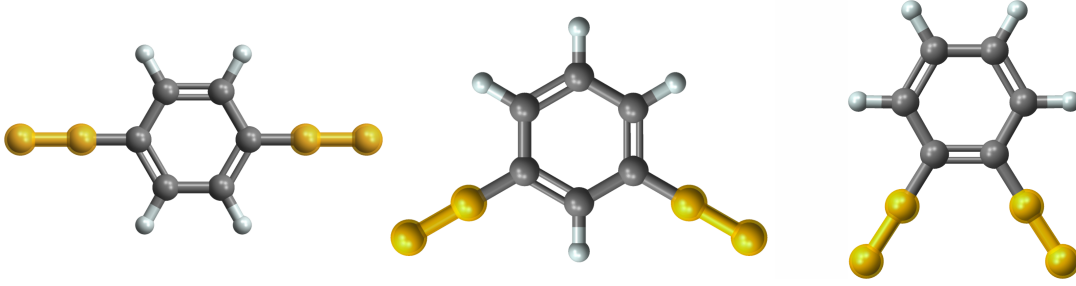


Figure 4.2: Benzene coupling configurations between two semi-infinite electrodes with gold parameterization. In para (left), meta (center) and ortho (right) configurations.

as show in Eqn. 4.16.

$$H_{1,4} = \begin{pmatrix} \varepsilon_0 + \left(\frac{t_s}{t_r}\right)^2 \Sigma & -t & 0 & 0 & 0 & -t \\ -t & \varepsilon_0 & -t & 0 & 0 & 0 \\ 0 & -t & \varepsilon_0 & -t & 0 & 0 \\ 0 & 0 & -t & \varepsilon_0 + \left(\frac{t_s}{t_r}\right)^2 \Sigma & -t & 0 \\ 0 & 0 & 0 & -t & \varepsilon_0 & -t \\ -t & 0 & 0 & 0 & -t & \varepsilon_0 \end{pmatrix}. \quad (4.16)$$

Then with this Hamiltonian we can calculate the Green's Functions by using Eqn. 4.11 and Eqn. 4.12. Finally, the transmission is calculated by using Eqn. 4.13, which is shown in Fig. 4.3. Following the same idea, we perform the calculation for the transmission of benzene in *meta* configuration by attaching the infinite chain terms on site 1 and 3 as shown in Eqn. 4.17 and with this Hamiltonian calculate the transmission, which is shown in Fig. 4.3.

$$H_{1,3} = \begin{pmatrix} \varepsilon_0 + \left(\frac{t_s}{t_r}\right)^2 \Sigma & -t & 0 & 0 & 0 & -t \\ -t & \varepsilon_0 & -t & 0 & 0 & 0 \\ 0 & -t & \varepsilon_0 + \left(\frac{t_s}{t_r}\right)^2 \Sigma & -t & 0 & 0 \\ 0 & 0 & -t & \varepsilon_0 & -t & 0 \\ 0 & 0 & 0 & -t & \varepsilon_0 & -t \\ -t & 0 & 0 & 0 & -t & \varepsilon_0 \end{pmatrix}. \quad (4.17)$$

Finally, we define another Hamiltonian for the *ortho* configuration by attaching the semi-infinite chain



terms on sites 1 and 2 as shown in Eqn. 4.18 and calculate the transmittance, which is shown in Fig. 4.3.

$$H_{1,2} = \begin{pmatrix} \varepsilon_0 + \left(\frac{t_s}{t_r}\right)^2 \Sigma & -t & 0 & 0 & 0 & -t \\ -t & \varepsilon_0 + \left(\frac{t_s}{t_r}\right)^2 \Sigma & -t & 0 & 0 & 0 \\ 0 & -t & \varepsilon_0 & -t & 0 & 0 \\ 0 & 0 & -t & \varepsilon_0 & -t & 0 \\ 0 & 0 & 0 & -t & \varepsilon_0 & -t \\ -t & 0 & 0 & 0 & -t & \varepsilon_0 \end{pmatrix}. \quad (4.18)$$

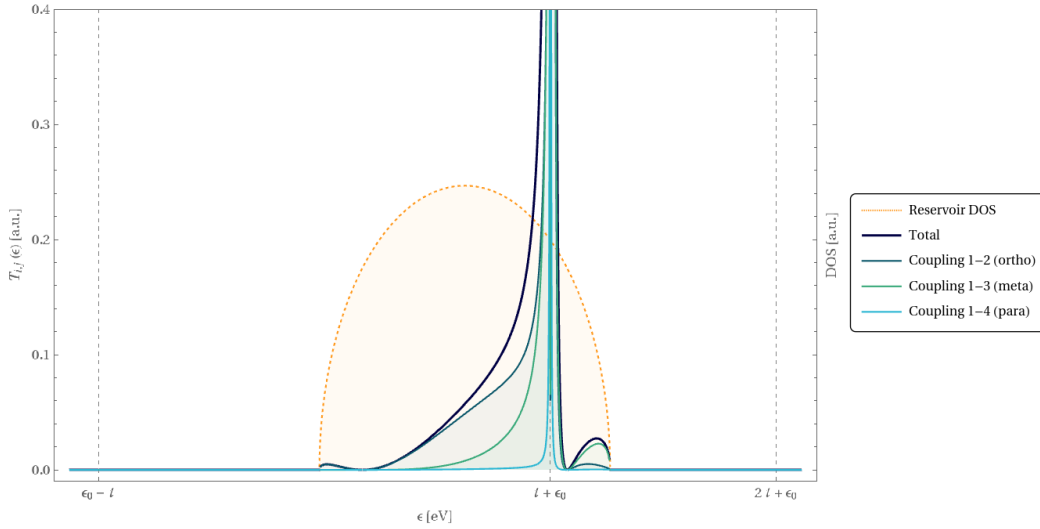


Figure 4.3: The plot shows the transmission through the benzene in the parallel configuration for the three different couplings. The light yellow region depicts the bandwidth of the gold contacts where transmission can occur. We see a concentration of the transmission around the LUMO level of the molecule widened and shifted by the self energy of the contracts. There are only slight differences between the ortho, para and meta configurations. The centers of the input and output bands differ by 1 meV. In this model the transmittance was calculated by making the contact of the infinite gold chain on an individual carbon atom, which is represented as the blue line. Then total transmittance is calculated by summing up the transmittance contribution of the 6 carbon atoms, which is represented as the dark blue line.

As it can be seen in Fig. 4.3, the transmittance changes depending on the site of the coupling. By comparing the transmittance between the different coupling, it can be seen that the coupling in *ortho* configuration can have transmission in a higher range of energy. The coupling in *meta* configuration has

transmittance in high range of energy, less than the *ortho* configuration and with less intensity. When the coupling occurs in the *para* configuration there is only transmittance in a tiny range of energy in the vicinity of the LUMO. All the coupling configurations have a very high transmittance in the vicinity of the LUMO level. It can also be observed that there is no transmission at HOMO level or at the highest energy level of molecule. For the *ortho* and *meta* it can also be concluded that there is more transmittance when the energy is lower than the LUMO level, when the energy is higher than the LUMO there is a small bump of transmittance that is higher for the coupling in *meta* configuration.

### Perpendicular coupling

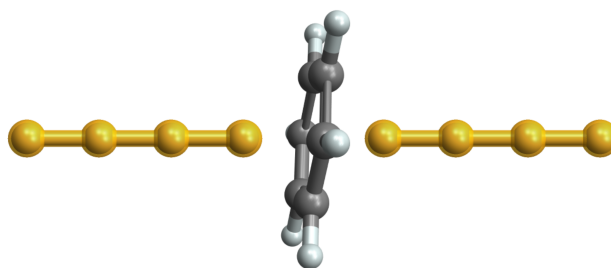


Figure 4.4: The plot shows the transmission through the benzene in the perpendicular configuration for a symmetric coupling to all carbons.

Another configuration that could occur is when the benzene molecule is perpendicular to the electrodes as shown in Fig. 4.3. To calculate the transmittance under this configuration we have to define a Hamiltonian, where both electrodes are attached on a single site, as shown in Eqn. 4.19. Then, we calculate the Green's function and the transmittance using the process described previously. The results of this calculation of an individual atom are plotted in Fig. 4.5. Then we have to attach the electrodes' contribution to the 5 remaining sites and perform the same transmittance calculations. Finally, we have to sum up the six individual transmittance of the 6 carbon atoms to obtain the total transmittance that occurs when the benzene molecule is attached to the electrodes in perpendicular configuration. The results of the

total transmittance are shown in Fig. 4.5.

$$H_{1,1} = \begin{pmatrix} \varepsilon_0 + 2\left(\frac{t_s}{t_r}\right)^2 \Sigma & -t & 0 & 0 & 0 & -t \\ -t & \varepsilon_0 & -t & 0 & 0 & 0 \\ 0 & -t & \varepsilon_0 & -t & 0 & 0 \\ 0 & 0 & -t & \varepsilon_0 & -t & 0 \\ 0 & 0 & 0 & -t & \varepsilon_0 & -t \\ -t & 0 & 0 & 0 & -t & \varepsilon_0 \end{pmatrix}. \quad (4.19)$$

As it can be seen in Fig. 4.5 when the benzene is coupled in perpendicular configuration, there is

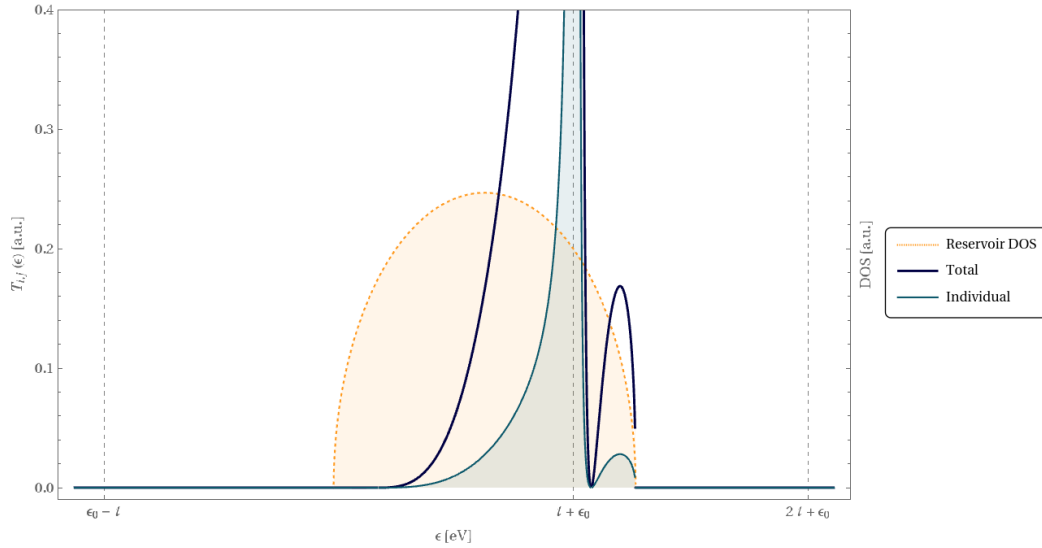


Figure 4.5: Benzene transmittance in perpendicular configuration. The light yellow region depicts the bandwidth of the gold contacts where transmission can occur. We see a concentration of the transmission around the LUMO level of the molecule widened and shifted by the self energy of the contacts. The centers of the input and output bands differ by 1 meV. The transmittance for this model was done by attaching the semi-infinite gold electrodes to an individual carbon atom, this individual transmittance is represented by the blue line. Then the total transmittance is calculated by summing up the transmittance of the 6 carbon atoms, which is represented by the thicker dark blue line.

transmittance in a big range of energy, almost in all the range of energy of the reservoir DOS. There exist a very high transmittance peak at the LUMO level, at lower energy from the LUMO level there is higher transmittance that reduces continuously. At higher energies than the LUMO there is a small bump of

transmittance with a small intensity.

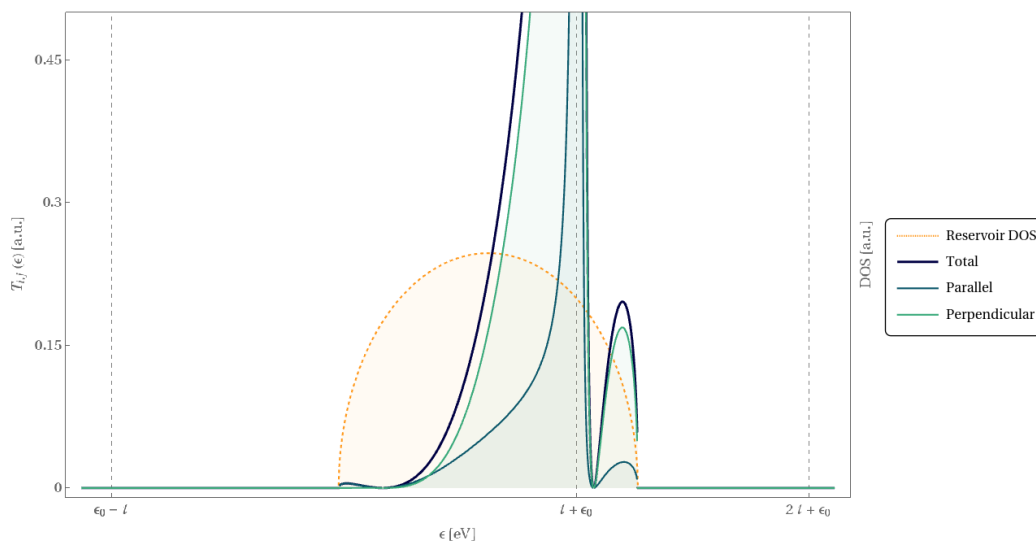


Figure 4.6: Comparison of benzene transmittance in perpendicular and parallel configurations. It can be observed that the transmittance in the perpendicular (green) configuration is higher than the transmittance in parallel (blue) configuration. Another observation that can be conclude is that the range of energy for the transmittance to occur is higher in the perpendicular configuration.

By comparing the total transmittance from all the configurations in the parallel configuration and the total transmittance through all the sites of the perpendicular configuration, as it can be observed in Fig. 4.6; the range of energy in the perpendicular configuration is much higher. This could explain why there is a higher conductance, shown in experiments<sup>7</sup>, under this configuration.

The theoretical approach presented before is just the beginning of a more thorough statistical analysis necessary to couple to experimental results. The benzene molecule can contact the electrodes in many configurations, and which ones are more probable must be captured with other theoretical tools (molecular dynamics). Nevertheless the transmission signature of the few configuration studied here appear very similar and will contribute to the histogram signature observed in the experiments.

## 4.2 Experimental measurements

The conductance measurements are performed at ambient conditions. To be able to make the measurement of a molecule, the MCBJ, has to be calibrated by making measurements of a clean gold wire. Then a solution of benzene is placed at the junction and the conductance measurements of benzene are recorded. All measurements are made by applying a  $V_{bias} = 101mV$  to the junction. This section presents the conductance measurements of a clean gold junction, amplifying the signal  $10^5$  and then presents the conductance histograms of benzene. Since the conductance of benzene is much lower, the signal is amplified  $10^6$  times.

### 4.2.1 Metallic measurements

For the gold conductance measurements, the conductance histograms are built by taking around 2000 conductance traces. An example of the collected traces can be observed in Fig. 4.7. The recorded traces plots show the signal in the form of *Conductance* ( $G_0$ ) vs. *Voltage ramp* ( $V$ ) applied to the piezoelectric. When we are amplifying the signal  $10^5$  the maximum conductance value is  $6.44 G_0$ , which result from the maximum output voltage of the IV preamplifier. As it can be observed in Fig. 4.7 conductance changes in multiple of  $G_0$ . After processing the collected traces a conductance histogram is built, which is shown in Fig. 4.8. The histogram is built by selecting the conductance points that fall between the range of  $4.9 G_0$  and  $0.2 G_0$  from every collected trace. As it can be seen in this histogram we have two very defined peaks, the first one at  $1 G_0$  and the other one at  $1.7 G_0$ . Comparing the histogram obtained with the result obtained by the research performed by Bramer Escamilla *et al.*<sup>3</sup> and the research performed by Costa-Krämer<sup>18</sup>, it can be observed that results from these measurements are located in very similar positions. From this results we can conclude that the MCBJ is making precise measurements, even if the number of points in a conductance plateau is very small.

Since the conductance of a benzene molecule is very small, we need to amplify the signal  $10^6$  times to be able to observe the signal. Before placing the benzene solution in the junction we performed the conductance measurements of clean gold to be able to compare these results with the measurements performed with benzene molecules. At the left from Fig. 4.9, it can be observed the conductance histogram of a clean gold junction by amplifying the signal  $10^6$  times. When the signal is amplified this amount the maximum conductance value is  $1.28 G_0$ . The conductance histogram is built after collecting around  $\sim 2000$  traces.

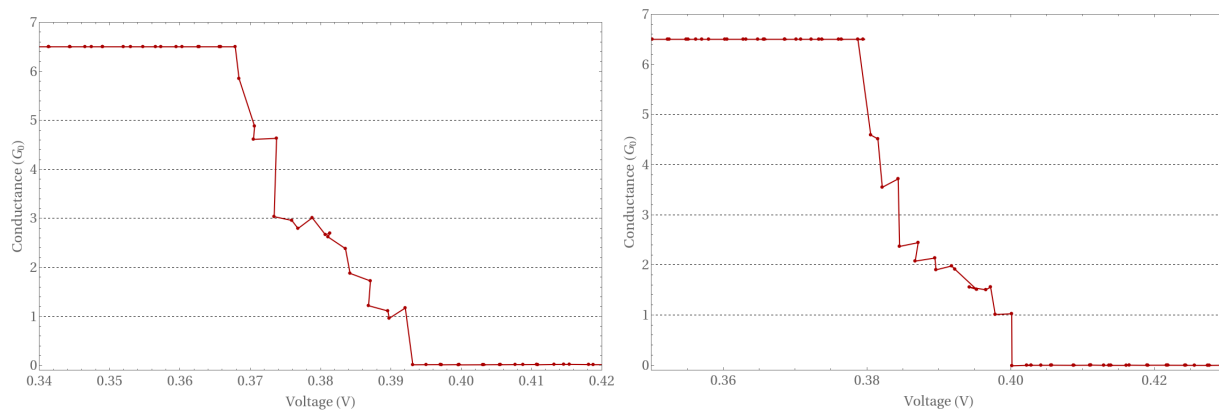


Figure 4.7: Example of gold conductance traces made at room temperature. The signal is amplified  $10^5$  times.

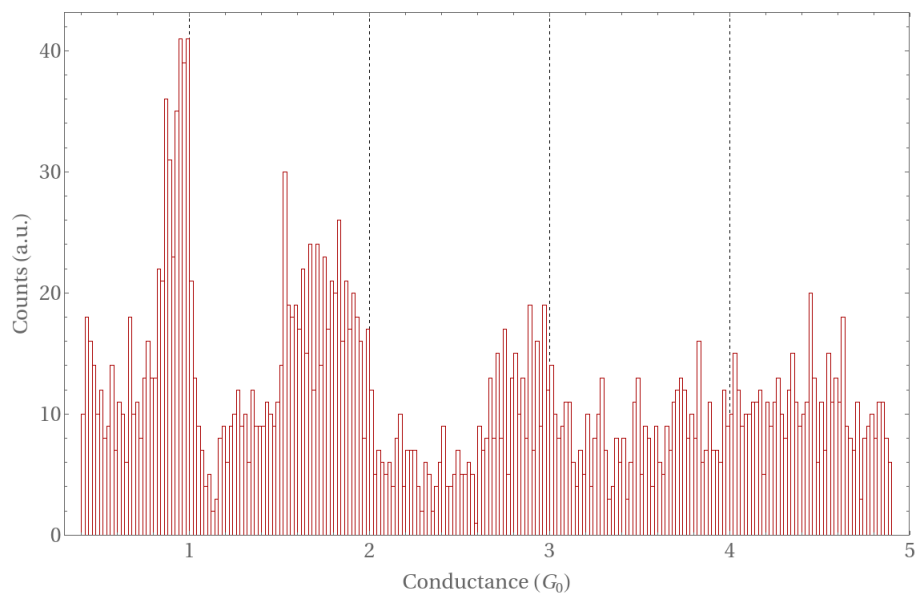


Figure 4.8: Gold conductance histogram.

Since the conductance of a benzene molecule is very small, an strategy used to be able to distinguished the conductance of molecules is to apply the logarithm to the conductance measurements and then with this information build the histogram. In order to be able to compare the conductance of benzene with conductance of clean gold at the right of Fig. 4.9 it can be observed the histogram of the logarithm of the conductance by applying a logarithmic scale in the  $y$ -axis. As it can be observed at the right of Fig. 4.9 we have the characteristic peak of gold at  $0 \text{ Log}(G_0)$ . Another characteristic that can be seen in this plot is that from  $-3.5 \text{ Log}(G_0)$  to  $-0.13 \text{ Log}(G_0)$  the conductivity decreases with a small slope, that when is plotted in logarithmic scale can be seen a constant linear decrease in the conductance.

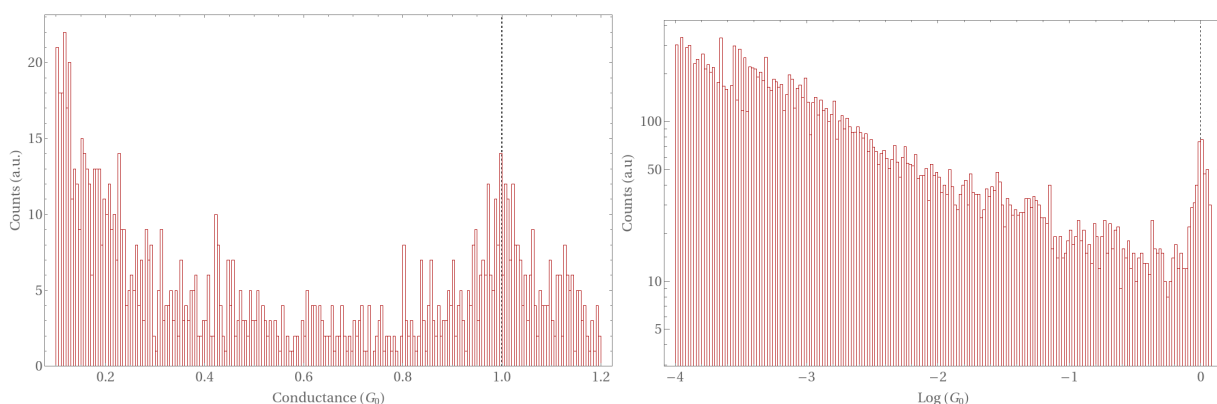


Figure 4.9: Gold conductance histogram amplifying the signal  $10^6$  times. To be able to distinguish low conductance values the conductance values and the counts of the histogram are plotted in logarithmic scale.

### 4.2.2 Molecules measurements

When the benzene drop is placed in the junction, it can be observed that the conductance histogram shape changes completely. One of the changes that it can be observed is that the conductance characteristic peak at  $0 \text{ Log}(G_0)$  is shifted to the right, to  $0.07 \text{ Log}(G_0)$ , which agrees to the results obtained by research performed by de Ara *et al.*<sup>7</sup>. Another important feature that shows the conductance of a benzene molecule is the peak at  $-0.30 \text{ Log}(G_0)$ , as it can be observed in Fig. 4.10. We are not able to observe the other characteristic conductance peaks since the resolution of MCBJ has to be improved. From region  $-1 \text{ Log}(G_0)$  to  $-2 \text{ Log}(G_0)$  there could be some signal that comes from benzene but since the resolution of the equipment is not good enough, benzene conductance gets mixed with the noise and we are not able to distinguish the

second peak at  $-1.98 \text{ Log}(G_0)^7$ . Another important characteristic of benzene in the conductance is that it has the effect of cleaning the sample, by reducing the interaction of particles in the environment with the junction; therefore reducing the noise and producing a much cleaner histogram. As it can be observed in Fig. 4.10 the shape of the histogram of benzene is completely different that the shape of clean gold. In the benzene histogram it can be observed that there is a more abrupt decrease in the conductance from  $-3 \text{ Log}(G_0)$  to  $-2.1 \text{ Log}(G_0)$ . After  $-2.1 \text{ Log}(G_0)$  the conductance keeps decreasing but with a less steeper slope until it reaches  $-1 \text{ Log}(G_0)$ , where we start to see an increase in the conductance until we reach it maximum point on  $-0.3 \text{ Log}(G_0)$  indicating the presence of benzene between the electrodes.

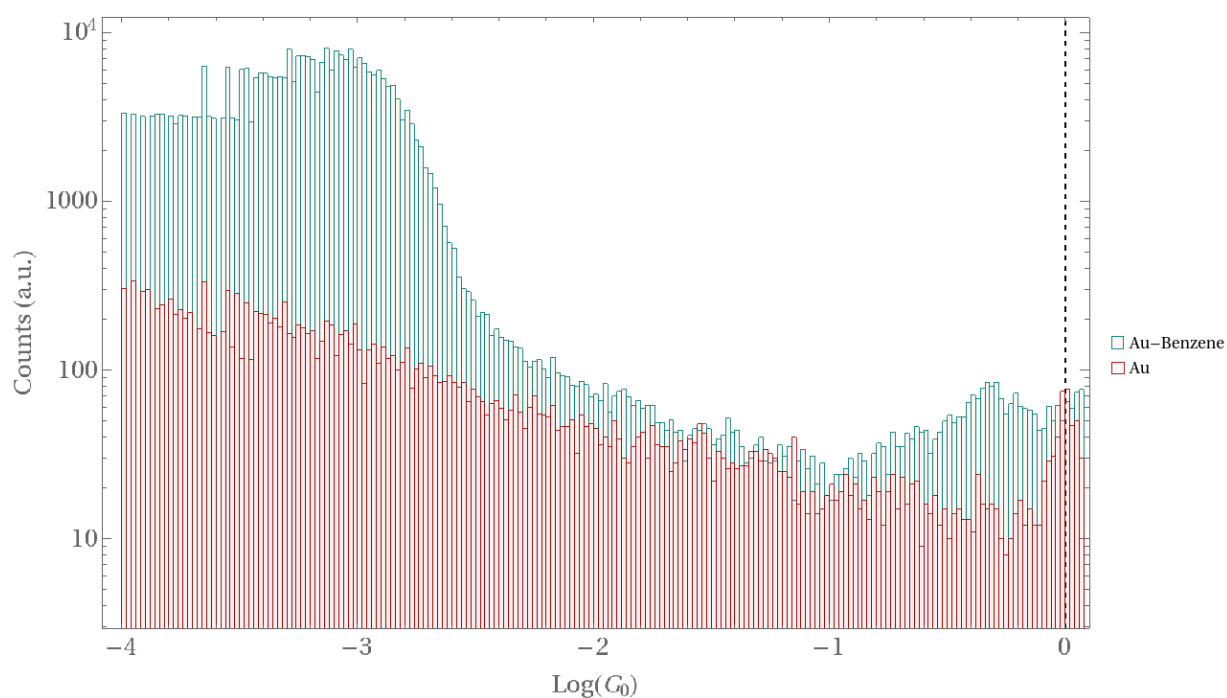


Figure 4.10: Comparison of clean Gold and Gold-benzene conductance histogram.





## Chapter 5

# Conclusion & Recommendations

Molecular electronics (ME) is a very promising research field of study with very exciting future applications. When the contact size between to electrodes is reduced, we start to observe the quantization of the conductance, which depends on the number of channels that can be occupied by the conducting electrons. By doing a tight binding model of a benzene molecule when coupled to a benzene molecule we showed the difference in the transmittance when the molecule is coupled in different configurations, as in experiments we expect a statistical mixture of the possible ways the molecules couple to both electrodes. The theoretical model includes the widening and shift of the conductance peaks due to the electrodes coupled to the molecule and how these peaks are related to the spectrum of the molecule (HOMO-LUMO levels). We found that the benzene molecule has transmission maxima in the vicinity of the LUMO level which is well captured within the bandwidth of the gold contacts. There are a few factors that are unknown to parameterize the model since no linking molecules are used and so the the molecules are bound to the contacts by weak forces. Experimentally there are some configurations that are more probable than others, in the theoretical model these more probable configurations have to be considered in order to have a closer similarity with experiments.

In this research we performed the measurement of the conductance of a clean gold junction by using the Mechanically Controlled Break Junction (MCBJ) technique at ambient conditions. After collecting around  $\sim 2000$  traces we were able to build a conductance histogram of clean gold junction where it can be observed the characteristic gold conductance peaks at  $1 G_0$  and  $1.7 G_0$ , which shows the conductance quantization in a gold junction. Since the conductance of a molecule is much smaller than the conductance of a metal junction, one needs first to measure the resolution of the MCBJ equipment. We determined that

the average resolution of the equipment, at  $0 G_0$ , has a standard deviation of  $0.001 G_0$ , and a maximum and minimum value of  $-0.003 G_0$  and  $0.003 G_0$  respectively. From the measured resolution it was determined that the conductance of a molecule needs to be higher than  $0.003 G_0$  to be able to be detected without being affected by the electrical noise of the equipment. For the current resolution of the equipment it was decided that a good molecule that could be measured is benzene. To be able to observe the low conductance values, one strategy that is used is to apply the logarithm to the conductance values and then build the histogram. By performing the measurements of benzene and building the histogram, we found that this molecule has the property of shifting the gold peak a little to the right and also has its conductance peak at  $-0.30 \text{ Log}(G_0)$ . Another important feature that was observed was that benzene had the property of cleaning the junction reducing the noise caused by the environment.

For future experiments some of the improvement that could be made are the transferring of the circuit of the preamplifier into a circuit board. This improvement will reduce the electrical noise of the equipment, therefore increasing its resolution. This improvement will allow us to perform measurements of molecules with a much lower conductance, such as biphenyl molecules which is well studied molecule. Another improvement that could be made is the implementation of an offset on the piezoelectric in order to have more control in the breaking and forming cycles of a wire.

# Bibliography

- [1] Scheer, E.; Cuevas, J. C. *Molecular electronics: an introduction to theory and experiment*; World Scientific, 2017; Vol. 15.
- [2] Tao, N. J. *Nanoscience And Technology: A Collection of Reviews from Nature Journals*; World Scientific, 2010; pp 185–193.
- [3] Bramer Escamilla, W.; López, A.; Borja Espinosa, C. N. Conductance measurements on atomic-sized contacts of gold using a low-cost mechanically controllable break junction equipment. Ph.D. thesis, Universidad Yachay Tech, 2020.
- [4] Agrait, N.; Yeyati, A. L.; Van Ruitenbeek, J. M. Quantum properties of atomic-sized conductors. *Physics Reports* **2003**, *377*, 81–279.
- [5] Ludoph, B.; Van Ruitenbeek, J. Conductance fluctuations as a tool for investigating the quantum modes in atomic-size metallic contacts. *Physical Review B* **2000**, *61*, 2273.
- [6] Ott, F.; Barberan, S.; Lunney, J.; Coey, J.; Berthet, P.; de Leon-Guevara, A.; Revcolevschi, A. Quantized conductance in a contact between metallic oxide crystals. *Physical Review B* **1998**, *58*, 4656.
- [7] de Ara, T.; Sabater, C.; Borja-Espinosa, C.; Ferrer-Alcaraz, P.; Baciú, B.; Guijarro, A.; Untiedt, C. Molecular Electronic Transport at Ambient Conditions of Adsorbed Organic Solvents. *The Journal of Physical Chemistry C (Under review)*
- [8] Saxena, V.; Malhotra, B. Prospects of conducting polymers in molecular electronics. *Current Applied Physics* **2003**, *3*, 293–305.
- [9] others,, *et al.* Electric-field induced bistability in single-molecule conductance measurements for boron coordinated curcuminoid compounds. *Chemical science* **2018**, *9*, 6988–6996.

- [10] Sjulstok, E.; Olsen, J. M. H.; Solov'yov, I. A. Quantifying electron transfer reactions in biological systems: what interactions play the major role? *Scientific reports* **2015**, *5*, 1–11.
- [11] Chen, F.; Hihath, J.; Huang, Z.; Li, X.; Tao, N. Measurement of single-molecule conductance. *Annu. Rev. Phys. Chem.* **2007**, *58*, 535–564.
- [12] Žutić, I.; Dery, H. Taming spin currents. *Nature materials* **2011**, *10*, 647–648.
- [13] Žutić, I.; Fabian, J.; Sarma, S. D. Spintronics: Fundamentals and applications. *Reviews of modern physics* **2004**, *76*, 323.
- [14] Bogani, L.; Wernsdorfer, W. *Nanoscience and technology: a collection of reviews from nature journals*; World Scientific, 2010; pp 194–201.
- [15] Wang, L.; Wang, L.; Zhang, L.; Xiang, D. Advance of mechanically controllable break junction for molecular electronics. *Molecular-Scale Electronics* **2019**, 45–86.
- [16] Neamen, D. A. *Semiconductor physics and devices: basic principles*; New York, NY: McGraw-Hill,, 2012.
- [17] van Ruitenbeek, J. M. *Metal Clusters at Surfaces*; Springer, 2000; pp 175–210.
- [18] Costa-Krämer, J. Conductance quantization at room temperature in magnetic and nonmagnetic metallic nanowires. *Physical Review B* **1997**, *55*, R4875.
- [19] McCreery, R. L.; Bergren, A. J. Progress with molecular electronic junctions: meeting experimental challenges in design and fabrication. *Advanced materials* **2009**, *21*, 4303–4322.
- [20] others,, *et al.* Solid state physics. 1976.
- [21] Pastawski, H. M.; Medina, E. Tight Binding' methods in quantum transport through molecules and small devices: From the coherent to the decoherent description. *arXiv preprint cond-mat/0103219* **2001**,
- [22] Atkins, P. W.; Friedman, R. S. *Molecular quantum mechanics*; Oxford university press, 2011.
- [23] Kucharczyk, R.; Davison, S. Effect of molecular wires attached to benzene: Local density-of-states study. *Physical Review B* **2004**, *69*, 195402.

- 
- [24] Harrison, W. A. *Electronic structure and the properties of solids: the physics of the chemical bond*; General Publishing Company, 1989.
- [25] Hinkle, A. R. Tight-binding calculation of electronic properties of oligophenyl and oligoacene nanoribbons. **2008**,
- [26] McMurry, J. E.; Fay, R. C.; Robinson, J. K. *Chemistry*; Pearson Education, Inc., 2015.



# Abbreviations

**ADC** analog-to-digital converter 21

**AFM** Atomic Force Microscope xi, 3, 4, 6

**CPs** Conducting Polymers 7

**DAQ** data acquisition xii, 30, 32, 33

**DOS** density of states 45, 50

**HOMO** Highest occupied molecular orbital xiii, 27, 28, 42, 44, 49

**LCAO** linear combination of atomic orbitals 41

**LUMO** lowest unoccupied molecular orbital xiii, 27, 28, 42, 44, 49, 50

**MCBJ** Mechanically Controlled Break Junction v, vii, ix–xiii, 4, 5, 7, 9–11, 19, 20, 29–35, 37, 38, 52, 54, 57

**ME** Molecular electronics v, vii, ix, xi, 1, 2, 7, 11, 57

**PZT** Piezoelectric Transducer 4, 5

**RAM** Random Access Memory 7

**SALC** symmetry-adapted linear combinations 44

**SERS** Surface-enhanced Raman Scattering 10

**STM** Scanning Tunneling Microscopy xi, 3–6

**SWCNTs** Single Walled Carbon Nanotubes 9